# BIOCHAR AMENDMENT FOR ENHANCED INFILTRATION AND AGGREGATION OF COMPACT URBAN SOILS

by

Sraboni Chowdhury

A thesis submitted to the Faculty of the University of Delaware in partial fulfillment of the requirements for the degree of Master of Civil Engineering.

Spring 2021

**BIOCHAR AMENDMENT FOR ENHANCED INFILTRATION AND AGGREGATION OF COMPACT URBAN SOILS**

by

Sraboni Chowdhury

Approved: _____
Paul T. Imhoff, Ph.D.
Professor in charge of thesis on behalf of the Advisory Committee

Approved: _____
Jack Puleo, Ph.D.
Chair of the Department of Civil and Environmental Engineering

Approved: _____
Levi T. Thompson, Ph.D.
Dean of the College of Engineering

Approved: _____
Louis F. Rossi, Ph.D.
Vice Provost for Graduate and Professional Education
Dean of the Graduate College

## ACKNOWLEDGMENTS

I would like to give my utmost gratitude to my beloved mother Karuna Chowdhury, whose nurturing and sacrifices have paved my way of progression to this point. I would also like to express my sincerest gratitude to my advisor, Professor Paul Thomas Imhoff for his consistent guidance, insights and continual support and motivation throughout the whole journey. I am grateful to my lab mates Derya Akpinar and Seyyedaliakbar Nakhli. It was a great opportunity to work with them and learn from them. My gratitude to all the graduate and undergraduate students, Marcus Bowser, Kai Kang, Reid Williams, Elizabeth Shepherd and Eric Noe for their help during field data collection. Besides, I acknowledge the funding agencies, National Fish and Wildlife Foundation, Howard Ecoworks, Maryland Transportation Authority and Delaware Department of Transportation. My last but not the least gratitude to my husband, Joyanta Debnath and all other close family members and friends, including my father and elder sister.

## TABLE OF CONTENTS

## LIST OF TABLES

## LIST OF FIGURES

## ABSTRACT

Urban development results in soil compaction and conversion of pervious lands into impervious surfaces, which decreases soil infiltration and increases stormwater runoff volume and associated pollutants. To alleviate the problem, biochar – a porous carbonaceous material – may be amended to existing soils next to impervious surfaces such as parking lots and roadways to increase stormwater infiltration. To assess the impact of biochar amendment at the field scale, a commercial wood-based biochar was amended with soil adjacent to urban impervious surfaces at four sites- two sites receiving stormwater runoff from parking lots and two sites from Interstate-95. The effectiveness of biochar to enhance stormwater infiltration in test sites was assessed periodically up to 1.5 years by measuring saturated hydraulic conductivity ($K_{sat}$). Factors affecting soil $K_{sat}$ such as soil compaction, vegetation density, soil water retention capacity, water-stable aggregate fraction and organo-mineral content were measured in undisturbed field soil cores at different ages (up to five months for highway soils and up to 15 months for parking lot soils) of the treatment systems. Results showed that despite the spatial (soil texture) and temporal (season) variability, the geometric mean $K_{sat}$ of 4% (w/w) biochar amended soils was 1.8 to 4.6 times greater than that of undisturbed soils. The building blocks of water-stable aggregates, the organo-mineral content, in 4% biochar amended soils were on average 1.7 times and 3.9 times higher than undisturbed soils after five months and 16 months, respectively. Consistent with these data, water stable aggregate fractions in 4% biochar amended soils were on average 27.2% and 47.3% greater than in undisturbed soils after five months and 16 months, respectively. For the first time, this study showed that biochar is effective in enhancing infiltration in compact roadway soils causing increased hydraulic conductivity, improved water retention and improved soil structure through biochar mediated aggregation.

# Chapter 1

# INTRODUCTION

Urban development is the process of converting natural pervious soils (forests, grassland, other vegetated surfaces) into urban land use with impervious surfaces such as parking lots, roadways, and rooftops. This process involves removal of vegetated surface soil exposing subsurface soil with poorer drainage characteristics, import of different soils for topsoil, and subsequent compaction associated with soil placement, grading, and movement of heavy construction traffic (Chen et al., 2014; Olson et al., 2013; Pitt et al., 2009). In addition, the disturbances during construction adversely influence soil structure leading to increased bulk density, disrupted aggregation, and reduced pore space, thus changing soil hydraulic properties (Chen et al., 2014). Consequently, the infiltration characteristics of urban soil, which are closely related to soil structure (Chen et al., 2014a), are adversely affected and usually result in increased stormwater runoff volume and associated pollutant flux from the urban watershed (Ahmed et al., 2015; Olson et al., 2013).

To alleviate the problem, biochar – a pyrogenic carbonaceous material produced from the thermochemical conversion of biomass under oxygen limited environment, known as pyrolysis, can be amended to existing soil next to urban impervious surfaces. Several studies have reported biochar's potential to alter key soil properties - bulk density, particle size distribution, and porosity including pore size and pore connectivity (Masiello et al., 2015). Such biochar-driven changes can directly affect soil hydrologic properties such as saturated hydraulic conductivity and water holding capacity. Among key soil hydraulic properties, the saturated hydraulic conductivity ($K_{sat}$) controls

partitioning of rainfall into surface runoff and water infiltration into the soil profile (Voter & Loheide, 2018). Thus, increasing soil saturated hydraulic conductivity is a critical task for enhancing stormwater infiltration and reducing runoff volume and associated pollutant loading from urban soils.

Biochar amendment has been reported to increase, decrease, or have no effect on $K_{sat}$ depending on the biochar type, amount applied, and the soil that the biochar is amended to. Based on data from 24 studies, Omondi et al., (2016) found that biochar amendment increased $K_{sat}$ for coarse (USDA soil texture sandy loam, sandy clay loam, loamy sand, and sand), medium (loam, silt loam, and silt), and fine (clay, clay loam, silty clay loam, and silty clay) textured soil. On the other hand, based on 28 datasets, Blanco-Canqui and Humberto (2017) reported that biochar amendment increased $K_{sat}$ in fine soils (loam, silt loam, silty clay loam, and clay), had limited or no affect in medium textured soil, but decreased $K_{sat}$ in coarse soils (coarse sand, sand, fine sand, and sandy loam). Using an even larger dataset of 61 studies, Edeh et al., (2020) found that biochar amendment reduced $K_{sat}$ in coarse soils (sandy loam, loamy sand, and sand), but increased $K_{sat}$ in medium (loam, silt loam, clay loam, and silty clay loam) and fine textured soils (clay and silty clay). Based on these meta-analyses, the impact of biochar on $K_{sat}$ is highly variable with contradictory results reported in the literature. In addition, most of the data in these studies were obtained from laboratory column experiments or greenhouse studies, where either immediate or short-term effects were monitored with few field-scale, long-term studies. Without a clear understanding of the long-term effects of biochar amendment on $K_{sat}$, it is not possible to confidently recommend biochar as a soil amendment to increase stormwater infiltration.

The effect of biochar on soil $K_{sat}$ and other hydraulic properties can be better understood and implemented if the controlling factors that alter the soil hydrology are understood. The immediate effect of biochar amendment on soil might be explained

with how biochar properties (particle size, shape, porosity or density) alter the intra- and interparticle pore network, changing the water movement in a soil matrix (Lim et al., 2016; Liu et al., 2016). However, over time, both intra- and inter-particle pores may be filled with soil minerals and microbes after extended exposure in a soil environment, thus triggering long-term changes in soil water dynamics including soil aggregation (Masiello et al., 2015). Improved soil structure marked by higher aggregation and enhanced porosity plays an important role in retention and transmission of water in soil resulting in increased infiltration and reduced runoff (Bronick & Lal, 2005; Regelink et al., 2015; Z. Zhang et al., 2016) Several studies have reported the potential of biochar to enhance soil aggregation and processes affected by aggregation (Kelly et al., 2017; Obia et al., 2016; Rahman et al., 2018; Q. Zhang et al., 2020; Zheng et al., 2018).

Soil aggregates are secondary particles formed overtime thorough interaction of minerals with organic substances bonded into organo-mineral complexes. The formation of organo-mineral complexes depends on the soil properties such as soil texture, organic matter content, mineral composition, soil pH, cation exchange capacity, exchangeable ions, moisture availability and microbial activities (Bronick & Lal, 2005; Regelink et al., 2015). Being a Particulate Organic Matter (POM), biochar particles of 0.25 - 2 mm can work as a formation or precipitation nucleus for aggregate formation through complex interrelated physical, chemical and biological interactions with the soil matrix (Mukherjee & Lal, 2013; Yang et al., 2016). Biochar pH, being different from the soil pH, can trigger a number of soil processes leading to reaction between biochar and the soil phase. While initially the alkaline biochar can induce precipitation of oxide, hydroxide, phosphate, and carbonate mineral phases in soil, with time the stable aromatic functional groups of biochar undergoe oxidation forming more oxygen containing surface functional groups leading to surface acidity, negative charge and decreasing pH (Pignatello et al., 2019), which favors solubility of polyvalent cations

and adsorption of mineral and organic matter (Joseph et al., 2010; Pignatello et al., 2019; Regelink et al., 2015; Tisdall & OADES, 1982). Thus, organo-mineral complex formation involving the biochar oxidized surface, soil minerals and microbial biomass may take place providing resistance against further oxidation leading to stable soil aggregates (Mukherjee & Lal, 2013).

The time scales of processes controlling soil aggregation are poorly understood, and the ability to predict their effect on soil hydraulic properties is weak. Complicating our understanding of the impact of biochar, in the field additional factors affect soil aggregation and soil structure, including soil compaction, vegetation density, and plant species that may change with time and season (Ahmed et al., 2015). Field investigations that include natural environmental conditions would aid our understanding of biochar's impact on soil structure and $K_{sat}$ that are not possible in laboratory experiments. The objectives of the study were to (1) measure dynamic changes in $K_{sat}$ of roadway soils amended with biochar as they infiltrate urban stormwater runoff and associated pollutants; (2) evaluate the time-dependent changes in biochar's impact on $K_{sat}$ and soil aggregation, and (3) examine the correlation between these measurements and organo-mineral association, which is the fundamental process that biochar is hypothesized to influence.

# Chapter 2

# MATERIALS AND METHODS

## 2.1 Site Selection

Four sites were selected for the study to assess the impact of biochar amendment on stormwater infiltration and runoff reduction. Two locations representing dominant soil textures within the Tiber-Hudson watershed located in Ellicott City, Maryland, were selected for small-scale biochar amendment. The first site (Church site) is located adjacent to the St. Peters Episcopal Church (39$^{o}$26' N, 76$^{o}$80' W) parking lot and receives stormwater runoff from an 18 m wide asphalt-paved impervious surface. The second site (Slack site) is located adjacent to the Slack Funeral Home (39$^{o}$27' N, 76$^{o}$81' W) parking lot and receives stormwater runoff from a 27 m wide asphalt pavement. For large-scale assessment of roadway soil, two sites were selected along Interstate I-95. The first site (Ramp Site) is located along the 10 m wide asphalt exit ramp off I-95 southbound (SB) towards MD 279 northbound (NB) in Cecil County, Maryland (39$^{o}$64' N, 75$^{o}$80' W). The second site (Plaza Site) is along I-95 NB Adjacent to Tydings Bridge Toll Plaza (39$^{o}$59' N, 76$^{o}$07' W) that receives stormwater runoff from ~ 58 m wide concrete roadway. For all sites, in-tact soil cores (diameter 2.25 cm) were collected in 10 cm depth increments from the surface to 30 cm depth with a soil corer for initial evaluation of soil bulk density and texture.

## 2.2 Biochar Amendment Techniques

A commercial Rogue Biochar$^{TM}$, produced by Oregon Biochar Solutions (White City, OR, USA) was used for all sites. This biochar is made from tops and limbs of Douglas fir and Ponderosa pine and pyrolyzed at ~950$^{0}$C at a high heating rate. During the spring season, March 2019, two treatment strips each of 1.5 × 1.5 × 0.3 m (length × width × depth) were constructed at the Church and Slack Sites (Figure 2.1). The

treatment strips at these sites included Tilled with 0% and 4% biochar amendment (w/w). A sequence of steps was followed to construct the filter strips starting with the removal of the top 3 cm topsoil containing plant matter and grassroots using a hand shovel. Then the remaining soil in 0% and 4% sections were tilled to 30 cm depth using a rotary tiller. Following tilling, soils from each section were collected sequentially in buckets and placed in a plastic tarp and mixed with shovels and rakes to make a homogeneous soil mix. During mixing large rocks and cobbles were removed. Based on individual treatment strip volume and pre-installation field soil bulk density, the required mass of homogeneously mixed soil for 0% and 4% amended sections were determined. These masses were converted to an equivalent volume of dry biochar needed. Next, the required weight of soil and biochar, wetted with ~ 2 % (w/w) water to prevent air blowing and ensure homogenous mixing with soil (Nakhli, Goy, et al., 2021; Nakhli, Tian, et al., 2021) were placed in 10 cm depth increments and mixed with the rotary tiller, filling the 30 cm deep treatment sections in three lifts with soil only (for 0% amended section) and soil with biochar (for 4% amended section). After construction, sites were seeded with Tall fescue grass seed and stabilized with straw.

For the I-95 roadway sites, larger filter strips were constructed during the summer season, June 2020, with 0%, 2%, 4% biochar amendment (Figure 2.2). The constructions steps were similar starting with removal of top 3 cm soil using a CAT 279 compact track loader with a 78-inch smooth lip bucket. Then, the remaining soil up to 30 cm depth was tilled and mixed combining all sections (0%, 2%, and 4%) to make a homogenous soil mixture for the entire test region. A CAT 279 compact track loader attached with a Valentini Tiger 1800 harrow tiller, was used for tilling and homogenous mixing of soil-biochar up to 30 cm depth. This tiller with horizontal rotating prongs allowed uniform vertical and horizontal mixing throughout the 30 cm depth without inverting moist substructure soils. Also, the tiller was operated back and forth to ensure the horizontal homogenous mixing in the test sections. Based on pre-installation in-field

bulk density measurements, an equivalent amount of tilled soil was placed in 0% biochar amended sections to compensate for the topsoil removed. Next, the calculated amount (volume-based) of biochar was mixed in the biochar test sections in two steps. First, soil volume equivalent to 2% biochar (w/w) was removed to provide space for biochar addition and ensure uniform grading of the treatment sections and to prevent mounding of the biochar-soil mixture. Then, 2% by mass volume equivalent biochar was applied to the amended section's top surface and wetted with ~ 10 % (w/w) water followed by in-depth mixing of soil and wet biochar with the harrow tiller. Once 2% biochar was mixed with soil for the 2% and 4% test sections, an equivalent volume of 2% biochar amended soil was removed for the 4% test section, and additional biochar (wetted with additional ~10% water) was added and mixed following wetting, tilling and mixing to construct the 4% amended section. Following biochar amendment, sites were seeded at a rate of 5g/$m^2$ with a seed mixture of 70% Tall fescue and 30% annual ryegrass and stabilized with straw matting.

(a)

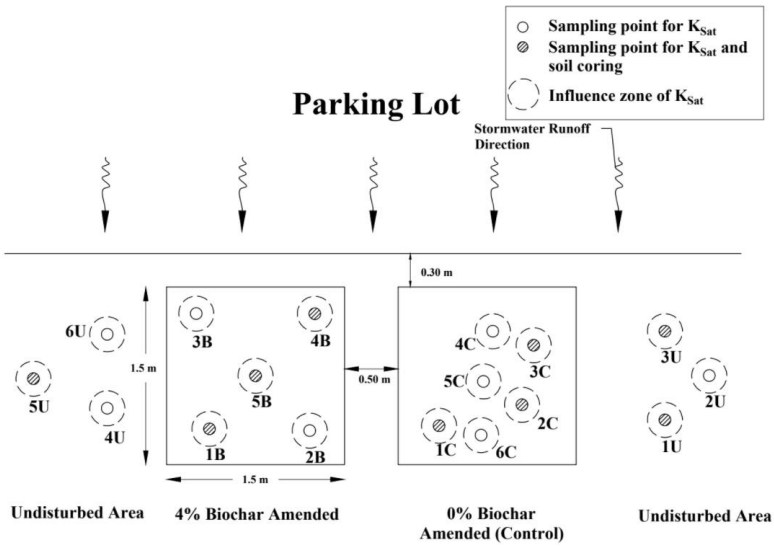


(b)

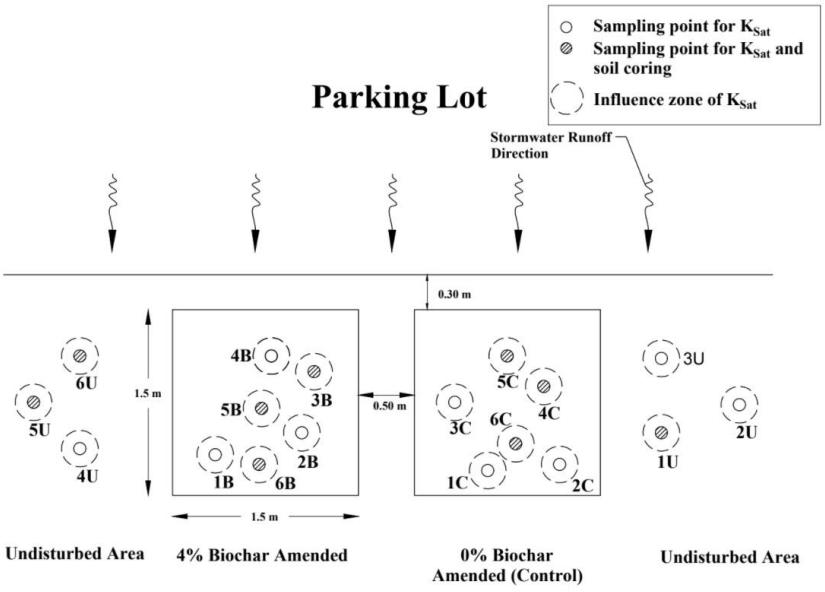


**Figure 2.1** Site plan showing field monitoring of $K_{sat}$ measurements during July 2020 for (a) Church Site (b) Slack Site. Numbers indicate sampling points. Letters indicate different treatment sections: U = undisturbed, C = 0% biochar amended(control), and B = 4% biochar amended.

(a)

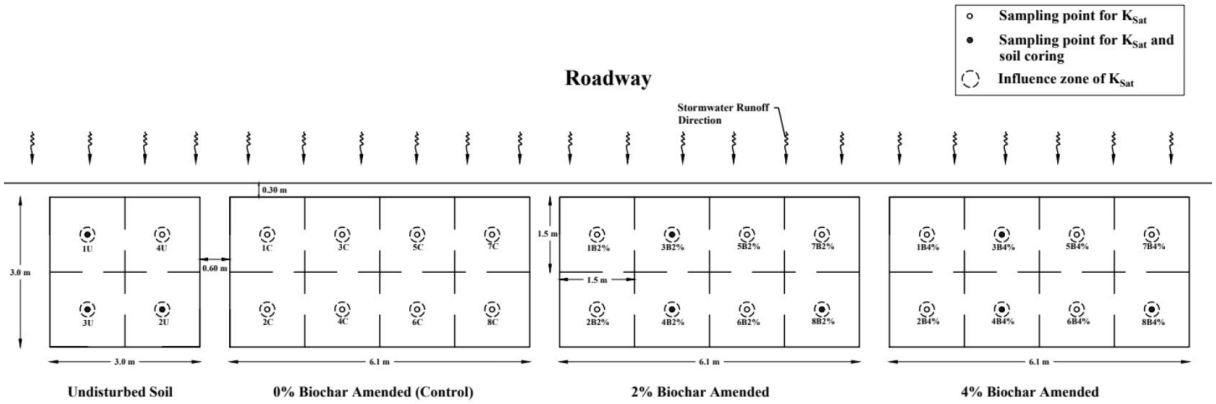


(b)

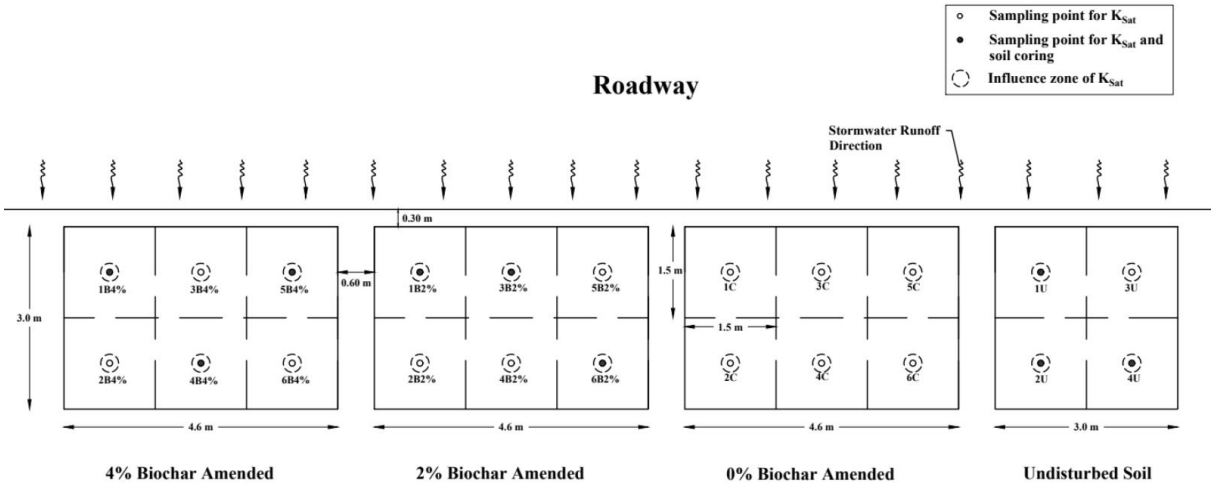


**Figure 1.2** Site plan showing field monitoring of $K_{sat}$ during November 2020 for (a) Ramp site and (b) Plaza Site. Numbers denote sampling points. Letters denote different treatment sections: U = undisturbed, C = 0% biochar amended (control), B2% = 2% biochar amended, and B4% = 4% biochar amended.

## 2.3 Soil and Biochar Characterization

A bulk sample of tilled homogeneous soil from each site and a composite sample of biochar from large super sacks used for treatment strip construction were collected during the construction period for physical and chemical characterization. Soil texture and particle density were determined following ASTM D433-63 and ASTM D854-14, respectively. Soil organic matter content was determined by the Loss on Ignition (LOI) method after heating at $550^0$ C for 24 hours. Soil and biochar pH were measured in 0.01 M $CaCl_2$ with a Hanna HI98194 pH meter (Hanna Instruments, Woonsocket, RI, USA) in solid-solution ratio of 1:2.5 for soil and 1:10 for biochar. For soil and biochar samples, surface area analysis was performed using Brunauer-Emmett-Teller (BET) analysis of $N_2$ adsorption isotherms acquired at 77.3K using Micromeritics ASAP 2020 (Micromeritics, Norcross, GA, USA). Measurements of surface area and elemental analysis for soil and biochar were performed at the Advanced Material Characterization Laboratory at the University of Delaware (Newark, DE,USA) Cation exchange capacity and exchangeable cations (Calcium (Ca), Potassium (K), Magnesium (Mg), Sodium (Na)) at pH 7 as well extractable nutrients (Phosphorus (P), Potassium (K), Calcium (Ca), Magnesium (Mg), Manganese (Mn), Iron (Fe), and Aluminum (Al)) were determined using the Mehlich 3 soil test extractant and analyzed by inductively coupled plasma optical emission spectroscopy using an ICAP 7600 Duo view Inductively Couple Plasma –Optical Emission Spectrometer (Thermo Elemental, Madison, WI, USA) The cation exchange capacity and extractable nutrient analyses were performed by the University of Delaware Soil Testing Lab (Newark, DE, USA) .All physical and chemical characterization measurements were performed in duplicate for each site soil and biochar samples.

## 2.4 Measurement of Field Saturated Hydraulic Conductivity

Periodic field testing was performed as described in Table 2.1 to quantify the field saturated hydraulic conductivity ($K_{sat}$) of biochar-amended and unamended soils. A Modified Phillip-Dunne (MPD) Infiltrometer (Upstream Technologies Inc, New Brighton, MN, USA) was used to measure $K_{sat}$ at multiple sampling points of individual treatment sections. For the smaller sites at Howard County, random sampling (Figure 2.1 and Figures A.1 and A.2, in Appendix A) was followed, while for larger sites sampling was conducted following a regular grid pattern within 1.5 × 1.5 m grid space (Figure 2.2 and Figure A.3 in Appendix A) to estimate the mean $K_{sat}$ of individual treatment sections.

**Table 2.1** Field scale monitoring plan

| Monitoring Task | Sites | Monitoring Period | Time Following Biochar Amendment |
|---|---|---|---|
| Field Saturated Hydraulic Conductivity | Church Slack | September 2019 | 5 months |
| | | November 2019 | 7 months |
| | | July 2020 | 15 months |
| | Ramp Plaza | August 2020 | 2 months |
| | | November 2020 | 5 months |
| Soil Compaction | Ramp Plaza | November 2020 | 5 months |
| Vegetative Cover | Ramp Plaza | November 2020 | 5 months |
| Undisturbed Soil Core Sampling | Church Slack | July 2020 | 15 months |
| | Ramp Plaza | November 2020 | 5 months |

For each measurement, the MPD infiltrometer was inserted 5 cm into the surface of the soil and then filled to a specified height (usually 30 cm) of water (Figure 2.3).

The change in water level in the MPD cylinder as it infiltrated into the ground was measured over time and recorded electronically with a wireless tablet.

(a)

(b)


**Figure 2.3** Field monitoring of saturated hydraulic conductivity ($K_{sat}$) using MPD infiltrometer at (a) Church site and (b) Plaza site.

For estimating $K_{sat}$ (cm/h), initial and final soil volumetric water content (% $cm^3/cm^3$), the penetration depth (5 cm) of the infiltrometer, and the water elevation relative to the soil surface (cm) versus time data (sec) were used. A Time Domain Reflectometer (TDR 150, Spectrum Technologies Inc., Aurora, IL, USA) was used in the field to measure the initial and final moisture content data calibrated following the procedure described in Wanniarachchi et al. (2019). The data collected from each infiltrometer measurement were analyzed via a spreadsheet utilizing the Visual Basic program to best-fit the water elevation versus time data according to procedures described elsewhere (Ahmed et al., 2014; Ahmed et al., 2015; ASTM D8152 -18).

## 2.5 Soil Compaction and Vegetation Cover

Soil compaction was measured (Figure 2.4) for the highway sites after five months of biochar amendment using a portable Static Cone Penetrometer (Model H-4210A, Humboldt Mfc.Co., Elgin, IL, USA) cone penetrometer. The cone had an area of 1.5 $cm^2$ and cone angle of $60^0$ and was pushed into the ground in 10 cm depth increments up to 30 cm. The mean average compaction pressure reading at each 10 cm interval was recorded. For each $K_{sat}$ sampling point, four measurements along the periphery of a 0.3 m square zone were averaged.

The percentage of vegetative cover for individual $K_{sat}$ sampling points was measured (Figure 2.4) within a wooden frame (30 × 30 cm) centered around the $K_{sat}$ sampling point. A nadir point digital photograph of the turfgrass cover, taken directly above the frame at a height of about 1m, was used to analyze the percent cover contributing to the sampling area using TurfAnalyzer (Green Research Services, LLC, Fayetteville, AR, USA) following procedures described elsewhere (Culpepper et al., 2020; Karcher & Richardson, 2005; Korres et al., 2019; Russell et al., 2019).

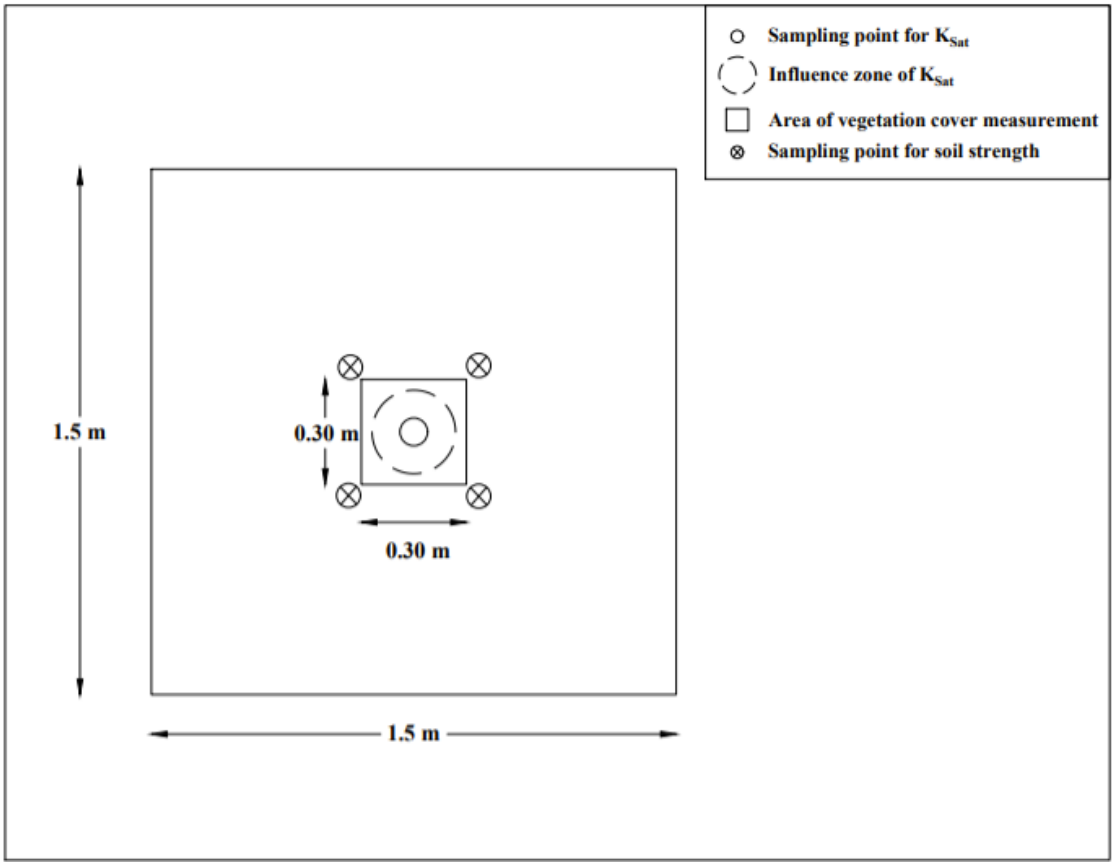


**Figure 2.4** Field plan showing soil compaction and vegetation cover measurement locations for an individual $K_{sat}$ sampling point.

## 2.6 Measurements Related to Water Retention and Soil Aggregation

Undisturbed soil core samples (8 cm diameter and 5 cm in height) below each MPD insertion point (5 cm) were collected in triplicates for each treatment (Figure 2.1 and Figure 2.2) at different ages of the site - after 15 months for Church and Slack site and after 4 months for Ramp and Plaza sites. These cores were used to evaluate soil water retention parameters using a pressure plate apparatus (Leong et al., 2004). The intact soil cores were first fully saturated with water and then placed on a pressure plate extractor for Field Capacity (FC) determination. Volumetric water content (% $cm^3/cm^3$)

at FC was determined by extracting water from undisturbed saturated samples at 0.33 bar until equilibrium was achieved. These samples were then oven dried at $105^0$ C for 48 hours. From oven dry weight, the dry bulk density was determined. Next, these samples were rewetted to a water content of FC+5%. An intact subsample (5 cm diameter and 2.5 cm height) of the rewetted samples were used for determining Permanent Wilting point (PWP) at 15 bar pressure, and the remaining soils were used for wet sieving analysis.

Wet sieving analysis was performed using 70 g equivalent dry soil and a series of three sieves to obtain > 2mm (large macroaggregate), 2-0.25 mm (small macroaggregate), and 0.25-0.053 mm (micro aggregate fraction) according to the procedure described elsewhere (Chen et al., 2014a; Denef et al., 2001; Six et al., 1998; Wick et al., 2009) The aggregate mass fraction of each size class was quantified and corrected for particle (sand and biochar) fraction according to the method described by Chen et al. (2014) and Wick et al. (2009). The particle corrected mean weight diameter (MWD) was calculated as follows.

$$MWD = \sum_{i=1}^{n} Mi \times Di \quad (2.1)$$

where $M$ (g/g) is the proportion of particle-corrected mass to the total sample dry mass, and $D$ (mm) is the arithmetic mean diameter of aggregate size fraction (5, 1.125, and 0.122 mm for large macroaggregate, small macroaggregate, and micro aggregate, respectively.

After performing wet sieving analysis, remaining soil samples from site-specific individual treatment sections were mixed and homogenized. Density fractionation using sodium polytungstate (SPT) solution was performed in duplicate using 10 g of those mixed and homogenized soil samples (< 2mm). Particulate organic matter (POM) fraction and organo-mineral associated fractions were separated using 1.6 g/cm$^3$ and 2.4 g/cm$^3$ SPT solutions, respectively, as described elsewhere (Brodowski et al., 2006; Pronk et al., 2012; Six et al., 1998).

## 2.7 Statistical Analysis

The one-way analysis of variance (ANOVA) with Tukey's honestly significant difference (HSD) post hoc test was used to compare means using a α -value of 0.05. Values of $K_{sat}$ are typically described as lognormal distribution (Ahmed et al., 2015); hence, log-transformed values of $K_{sat}$ were used for comparing the geometric means with Tukey's HSD test. The Pearson correlation coefficient (Pearson's r) was used to check the goodness of the linear relationship between variables. All statistical analyses were performed using JMP Pro 15 software.

# Chapter 3

# RESULTS

## 3.1 Physicochemical Properties of Soil and Biochar

The physicochemical properties of biochar and all sites soil are presented in Table 3.1. The biochar particles were larger than all site soils with fine gravel size (33.3 ± 1.3SE %) and sand size (66.7 ± 1.2 SE%) particles only. According to USDA classification, the soil texture for three sites (Slack, Ramp, Plaza) was loam and for the Church site was sandy loam. There was variability in particle size distributions between the sites. The gravel size particle content was highest for Slack site (25 ± 10 SE %) followed by roadway sites soils (~ 10% for Ramp and Plaza site) and was lowest (6.5 ± 0.1 SE %) for the Church site soil. The clay content was highest (16.0 ± 0.3 SE%) for Plaza site soil and was similar (~ 11%) for all other sites. The organic matter content for Church and Ramp site soils was lower (3.13 ±0.02 SE % and 3.32 ± 0.01 %, respectively) than Slack and Plaza site soils (5.54 ± 0.03% and 6.76 ± 0.02%). Among all sites, cation exchange capacity was lowest (8.3 ± 0.4 SE meq/100g) for the Ramp site soil. Exchangeable cation contents were lower for both Ramp and Plaza site soils (dominated by Na with on average 3.7 meq/100 g) than the Church and Slack site soils (dominated by Ca with on average 14.2 meq/100 g). Compared to the site soils, biochar had significantly higher surface area (553 ± 8SE $m^2$/g), organic matter content (88.8 ± 0.4 SE%), cation exchange capacity (54.6 ± 0.6), and exchangeable cations (dominated by Ca at 35.3 ± 0.1SE meq/100 g). Among the extractable nutrients, Ca content (mg/kg) was most abundant for all site soils, whereas for biochar K content (mg/kg) was dominant followed by Ca content (mg/kg). Biochar pH was alkaline, whereas except for the Slack site, all site soils were acidic. Biochar amendment increased (5.9 ± 0.2 SE % for 2% and 10.5 ± 0.5 % for 4% biochar amended soil) the soil pH initially for soil collected after five months from Ramp and Plaza sites. On the other hand, in the longer

duration tests in Howard County (collected after 15 months from Church and Slack sites), biochar amendment decreased (9.7 ± 1.5 SE% for 4% biochar amended soil) soil pH when compared to initial conditions and undisturbed soils. Such decreases in pH are likely related to the formation of acidic functional groups from oxidation or aging of biochar.

**Table 3.1** Physicochemical properties of Rogue Biochar™ and site soils. Values denote the mean (standard error of the mean) of duplicate measurements.

| **Parameter** | | **Rogue Biochar™** | **Church site soil** | **Slack site soil** | **Ramp site soil** | **Plaza site soil** |
|---|---|---|---|---|---|---|
| Particle size (% mass) | Fine gravel | 33.3 (1.3) | 6.5 (0.1) | 25 (10) | 10.9 (0.5) | 9.5 (0.8) |
| | Sand | 66.7 (1.2) | 54 (3) | 44 (6) | 39.5 (1.3) | 42 (3) |
| | Silt | - | 28.0 (1.8) | 19 (5) | 37.8 (1.5) | 32 (2) |
| | Clay | - | 11.4 (0.9) | 11 (5) | 11.8 (0.4) | 16.0 (0.3) |
| Particle density ($g/cm^3$) | Skeletal | 0.98 (-) | 2.63 (0.01) | 2.66 (0.01) | 2.71 (0.01) | 2.64 (0.02) |
| | Envelope | 0.44 (-) | | | | |
| BET surface Area ($m^2/g$) | | 553 (8) | 3.35 (0.01) | 3.20 (0.01) | 5.72 (0.01) | 9.94 (0.03) |
| Organic matter (% mass) | | 88.8 (0.4) | 3.13 (0.02) | 5.54 (0.03) | 3.32 (0.01) | 6.76 (0.02) |
| Cation exchange capacity (meq/100g) | | 54.6 (0.6) | 13.5 (0.2) | 18.2 (0.5) | 8.3 (0.4) | 13.1 (0.1) |
| Exchangeable cations (meq/100g) | Ca | 35.3 (0.1) | 11.1 (0.3) | 17.2 (0.1) | 1.89 (0.07) | 3.31 (0.08) |
| | K | 22.3 (0.1) | 0.13 (-) | 0.24 (-) | 0.07 (-) | 0.07 (-) |
| | Mg | 7.28 (0.01) | 0.84 (0.02) | 1.13 (0.01) | 0.29 (-) | 1.21 (0.02) |
| | Na | 11.18 (0.05) | 0.34 (-) | 0.03 (0.01) | 3.4 (0.2) | 3.9 (0.2) |
| Extractable nutrient (mg/kg) | P | 41.3 (0.5) | 27.20 (0.07) | 17.9 (0.4) | 16.8 (0.1) | 9.1 (0.1) |
| | K | 1024 (14) | 37.8 (1.2) | 86 (2) | 29.5 (0.5) | 24.6 (0.2) |
| | Ca | 749 (6) | 1635 (21) | 3381 (42) | 369 (4) | 574 (6) |
| | Mg | 128.2 (1.9) | 96.1 (1.1) | 136.7 (1.6) | 41.1 (0.8) | 134.6 (1.6) |
| | Mn | 29.9 (0.3) | 24.7 (0.1) | 37.2 (1.1) | 39.7 (0.4) | 30.2 (1.1) |
| | Fe | 49.0 (0.7) | 127.4 (1.2) | 71.7 (0.1) | 114.8 (1.1) | 91.3 (-) |
| | S | 32.7 (0.9) | 17.02 (0.21) | 26.9 (0.3) | 21.2 (0.3) | 19.6 (0.2) |
| | Na | 280 (4) | 40.4 (0.5) | 8.8 (0.1) | 704 (2) | 708 (4) |
| | Al | 53.6 (1.5) | 492 (3) | 215 (3) | 401 (5) | 626 (4) |
| pH | Initial | 9.5 (0.03) | 6.82 (0.02) | 7.54 (-) | 6.39 (0.01) | 6.09 (0.01) |
| | Final 0% | | 6.49 (0.01) | 6.96 (0.01) | - | - |
| | 2% | | - | - | 6.78 (0.04) | 6.44 (0.02) |
| | 4% | | 6.06 (0.04) | 6.92 (0.02) | 7.03 (0.02) | 6.76 (0.03) |

## 3.2 Field Saturated Hydraulic Conductivity

The saturated hydraulic conductivity ($K_{sat}$) measurements for different monitoring periods at different sites are presented in Figure 3.1 and tabulated in Table A.1 in Appendix A. For all sites, during the first monitoring period there was significant variability of $K_{sat}$ (coefficient of variation ranging from 0.4 to 1.8) with significantly higher mean (except Church site) of $K_{sat}$ for biochar amended soils.

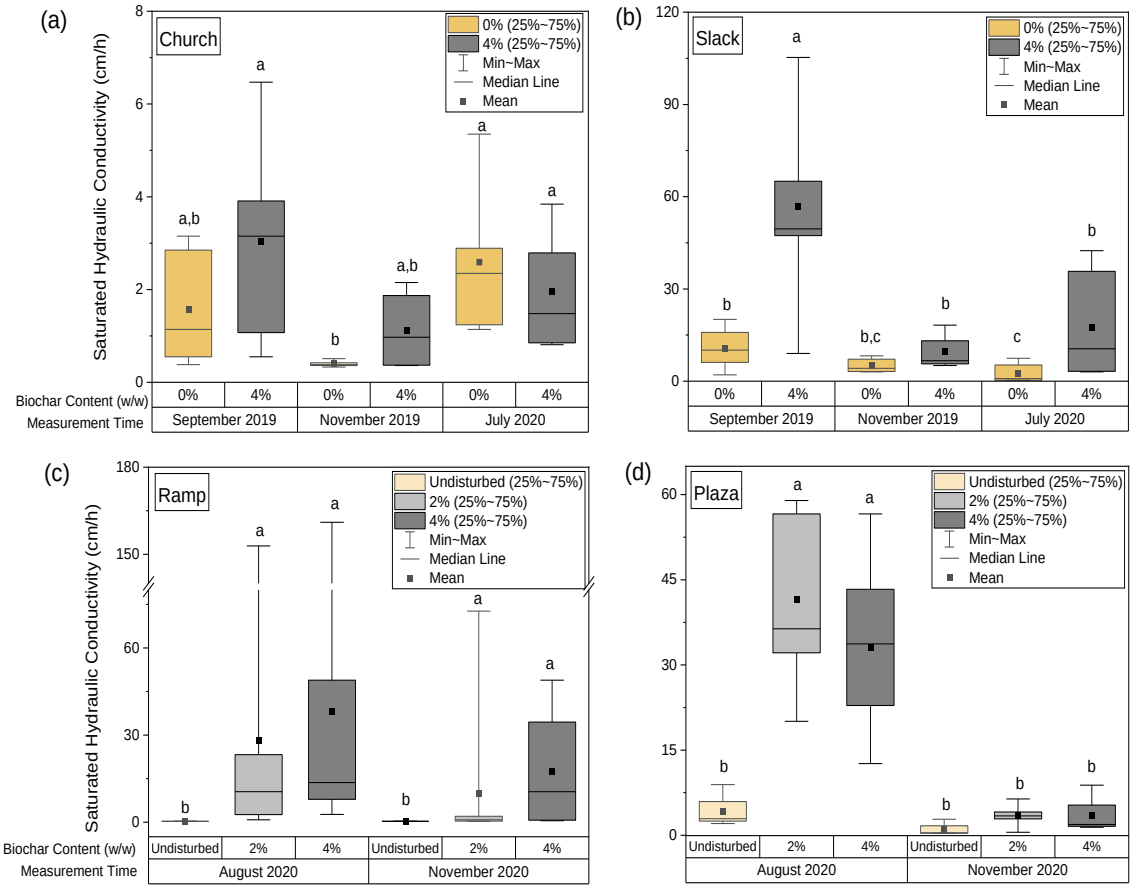


**Figure 3.1** Box plot showing field saturated hydraulic conductivity (cm/h) for different monitoring periods at (a) Church site, (b) Slack Site, (c) Ramp Site, and (d) Plaza site. Letters denote differences using Tukey's HSD test at $\alpha = 0.05$.

During the second monitoring period, variability of $K_{sat}$ decreased (coefficient of variation ranging from 0.17 to 1.0) in biochar amended soils except for the Plaza site and the 2% amended soil at the Ramp site. Irrespective of treatment, during the November monitoring period the $K_{sat}$ was lower at all sites, indicating the seasonal variability of field $K_{sat}$ likely associated with plant dynamics.

Despite the spatial and seasonal variability, the geometric mean $K_{sat}$ for 4% biochar amended soil in the Church site (Figure 3.1 (a) and Table A.1 in Appendix A) was ~ 2 times higher than the 0% amended soils except during the July 2020 period when vegetative species played a role that is discussed later. During the July 2020 period, the mean $K_{sat}$ in 4% amended area was 4.6 times higher than that of nearby undisturbed soil whereas mean $K_{sat}$ of 0% amended soil was 1.2 times higher than the nearby undisturbed soil (Table A.1 in Appendix A).

At the Slack site (Figure 3.1 (b)) and Table A.1 in Appendix A), the mean $K_{sat}$ of 4% amended soil was significantly higher than 0% amended soil except for the November 2019 testing period. Although during July 2020, it was found that biochar amendment had 30% lower mean $K_{sat}$ compared to the undisturbed soil that contained a high percentage of fine gravel size particle, which were partially removed from the treatment sections during construction.

At the Ramp site (Figure 3.1 (c) and Table A.1 in Appendix A), the $K_{sat}$ for undisturbed soil was < 0.3 cm/h for all sampling points regardless of season. Both 2% and 4% biochar amendment significantly increased the mean $K_{sat}$, which was ~ 2 times higher in 4% amended than 2% amended soils. Since the Ramp site test area had a slope of 30%, mean $K_{sat}$ for downslope sampling points in biochar amended sections were analyzed separately and were ~8-10 times higher than that of upslope soils during the first monitoring, two months after biochar amendment (Figure A.4 and Table A.2 in Appendix). During the second period of monitoring after five months of biochar amendment, the difference between upslope and downslope $K_{sat}$ decreased for 2%

amended sections (2.4 times higher in downslope soil) but significantly increased for the 4% amended section (47.7 times higher in downslope soils). The higher $K_{sat}$ in downslope soils may be attributed to overall decreased soil bulk density (Figure A.7 in Appendix A) with biochar amendment and probable erosion of biochar from upslope lodcations.

During the first monitoring period at the Plaza site (Figure 3.1(d) and Table A.1 in Appendix A), the mean $K_{sat}$ for both 2% and 4% treatments were significantly higher than undisturbed soil. Later, the mean $K_{sat}$ were not significantly different between 2% and 4% treatments yet 3.7 times and 5.3 times higher for 2% and 4% biochar amended soil, respectively, than the undisturbed soil. Although $K_{sat}$ were measured for several sampling points in 0% biochar amended section in both Ramp and Plaza site, due to soil cracking at the ground surface and preferential flow of water associated with this cracking (Figure A.5), $K_{sat}$ could not be reliably measured and thus are not reported.

### 3.3 Effect on Soil Water Retention

The mean field capacity (% $cm^3/cm^3$) and permanent wilting point (% $cm^3/cm^3$) measured with undisturbed soil cores collected at different treatment ages from different sites (Table 2.1) are shown in Figure 3.2. For all site soils, biochar amendment increased the field capacity (FC) and decreased the permanent wilting point (PWP).

The FC was significantly higher in biochar amended soils than the undisturbed soil for soil samples collected from Ramp and Plaza sites (Figure 3.2 (b)) after five months. For the Ramp site, the increase was 17.4% and 23.2% for 2% and 4% biochar amended soils, respectively. For the Plaza site, the mean FC was 38.2 % and 44.7% higher than undisturbed soils, for 2% and 4% biochar amended soils, respectively. For soil samples (collected after 15 months of biochar amendment), the mean field capacity in 4% biochar amended soils was 18.2 % higher in Church site and 15.7% higher in Slack site compared to undisturbed soils, whereas the increase for the 0% amended

(tilled only) soil was only 7.1% and 5.2% in Church and Slack sites, respectively (Figure 3.2 (a)).

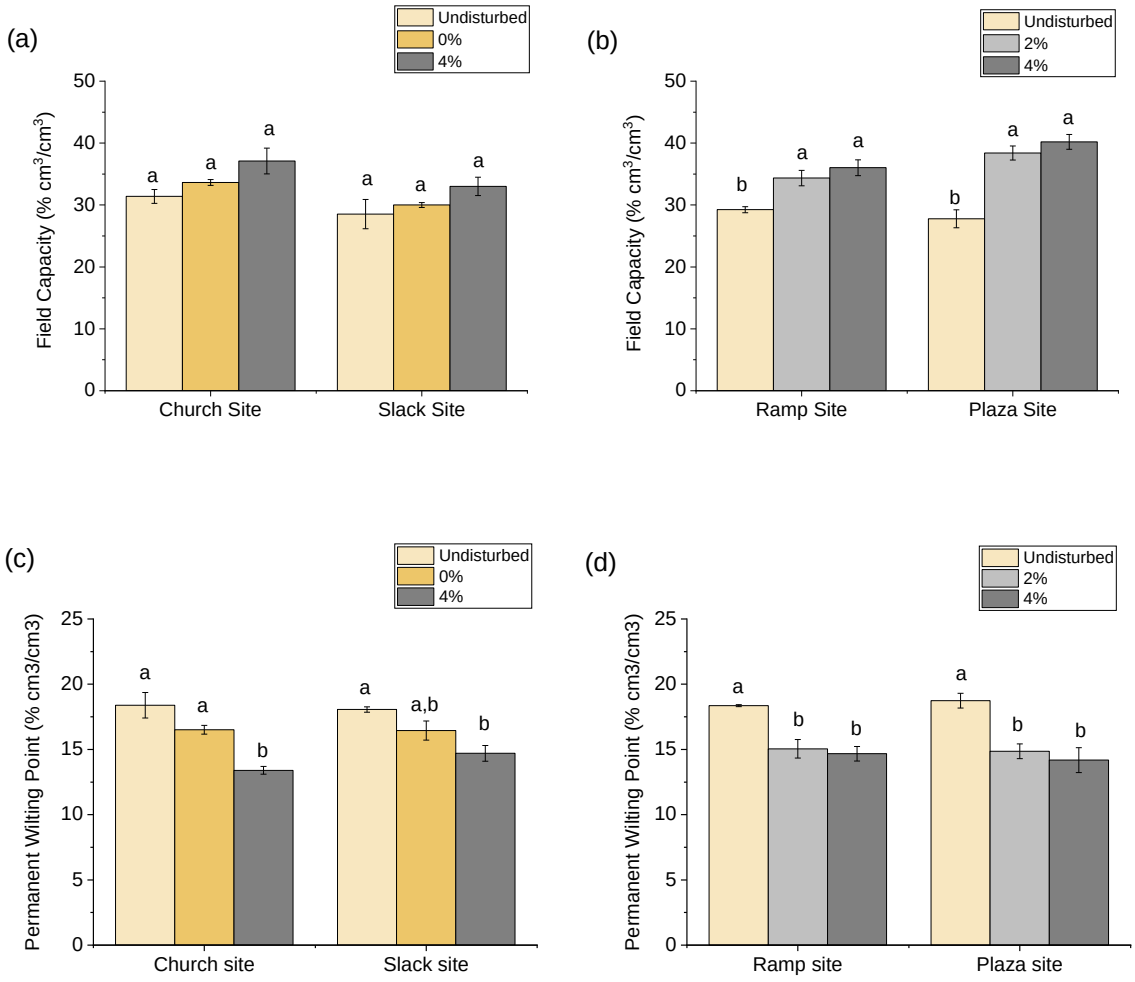


**Figure 3.2** Mean field capacity (% $cm^3/cm^3$) of soil samples collected from (a) Church and Slack sites after 15 months of biochar amendment, and (b) Ramp and Plaza sites after five months of biochar amendment. Mean permanent wilting point (% $cm^3$/cm3) of soil samples collected from (c) Church and Slack sites after 15 months of biochar amendment, and (d) Ramp and Plaza sites after five months of biochar amendment Error bars depict standard error of the means (n = 3 for all treatment). Letters denote differences using Tukey's HSD ($\alpha = 0.05$).

For all site soils, both 2% and 4% biochar amendment significantly decreased the PWP compared to undisturbed soils. For Church and Slack site soils (Figure 3.2(c)), mean PWP was on average 22 ± 4% lower in 4% biochar amended soils whereas the decrease was on average 9.6 ± 0.6% for 0% amended (tilled only) soils. For Ramp and Plaza site soils (Figure 3.2(d)), compared to undisturbed soil, mean PWP was on average 19.1 ± 1.1% and 22.6 ± 1.9SE% lower in 2% and 4% biochar amended soils, respectively. Due to cracking problem in Ramp and Plaza site, undisturbed soil cores for 0% treatment were not collected for water retention measurement.

### 3.4 Enhanced Soil Aggregation and Organo-Mineral Association

Soil aggregation is assessed by the water stable aggregate fraction, the mean weight diameter of all water stable aggregates, and the distribution of aggregates among different aggregate sizes. According to wide accepted aggregate hierarchy theory (Oades & Waters, 1991), soil aggregates are formed in a hierarchical manner meaning microaggregates act as smaller building blocks for small and large macroaggregates. The particle corrected fraction of different aggregate size fractions and the mean aggregate weight diameter for soils with different treatments at different sites are shown in Figure 3.4. As shown for all sites, 4% biochar amendment increased the mean aggregate fraction and the mean weight diameter of aggregates. The positive effect was highest for Church site soil and least for Plaza site soil.

For Church site soils (Figure 3.4 (a)), the mean fraction of total aggregates was 69.5% higher with a significantly higher fraction of large macroaggregate and 2.2 times higher mean weight diameter compared to the undisturbed soil. At the Slack site (Figure 3.4 (b)) where native soil is high in organic matter with high cation exchange capacity and exchangeable cations (Table 3.1), 4% biochar amendment increased the mean

fraction of total aggregates by 35.7% over undisturbed soil with 1.7 times higher mean aggregate weight diameter.

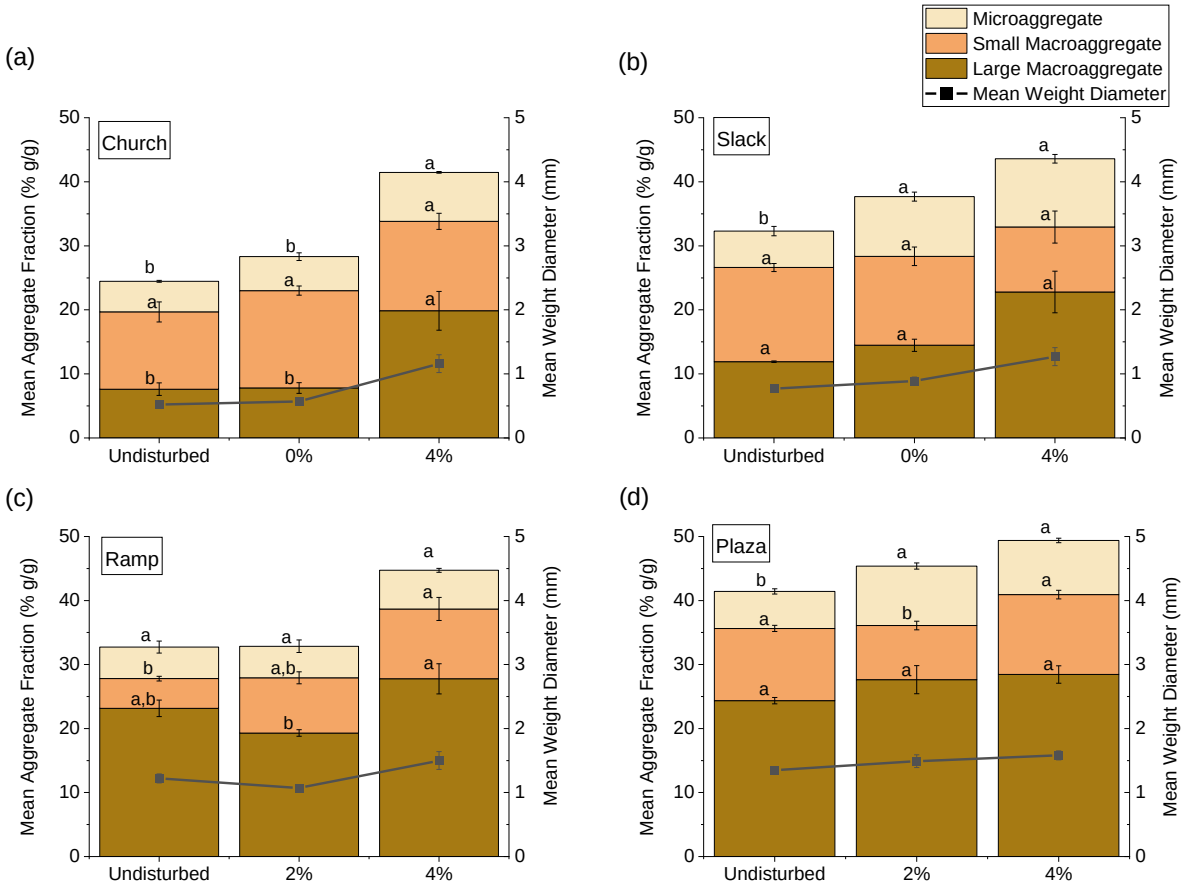


**Figure 3.4** Mean fraction (% g/g) of particle-corrected large macroaggregate (> 2mm), small macroaggregate (2-0.25 mm), microaggregate (0.25- 0.053 mm), and mean weight diameter (mm) of soil samples collected from (a) Church and (b) Slack sites after 15 months of biochar amendment, and (c) Ramp and (d) Plaza sites after five months of biochar amendment. Error bars depict standard error of the means (n = 3 for all treatment). Letters denote differences in each aggregate size fractions among treatments using Tukey's HSD test at $\alpha = 0.05$.

At the Plaza site (Figure 3.4 (d)), 4% biochar amendment increased the mean fraction of total aggregates by 19.3%. However, at the Ramp site where native soil is low in organic matter and cation exchange capacity is relatively small (Table 3.1), the 4% biochar amendment increased the mean fraction of total aggregate fraction by 35% within five months of biochar amendment. Since, reliable $K_{sat}$ could not be measured due to soil cracking in 0% treatment sections at the Ramp and Plaza sites, undisturbed soils cores were not collected for soil aggregation measurements.

Following amendment, biochar particles break up into smaller particles through fragmentation and disintegration. Such biochar particles can then act initially as a particulate organic matter and later form organo-mineral complexes acting as a precipitation nucleus of soil mineral microbes and organic matter. Hence, the fraction of particulate organic matter (POM) and mineral associated organic matter (organo-mineral complex or OM associates), hypothesized as the building block of stable aggregate formation, were measured to assess their correlation with mean aggregate fraction. Similar to the positive effects on aggregate fraction, the mineral associated organic matter (OM associates) fraction was significantly higher for 4% biochar amended soils in all sites with the most significant increase at the Church site and least at the Plaza site. For the Church site soil (Figure 3.5(a)), the fraction of OM associates was 7.6 ± 0.3SE % for amended soil, where for undisturbed soil it was only 1.5 ± 0.3SE%. For the Slack site where the fraction of the OM associates was higher (2.3 ± 0.2SE%) in undisturbed soil compared to the Church site, biochar amendment further increased the OM associates to 5.7 ± 0.1 SE%. At the Ramp and Plaza sites, an increased fraction of both particulate organic matter and OM associates were found with biochar amendment. For 4% biochar amended soil, at the Ramp site (Figure 3.5(c)) the mean fraction of OM associates was increased by 94.7% over undisturbed soil, while for the Plaza site soil it was increased by 40.6%.

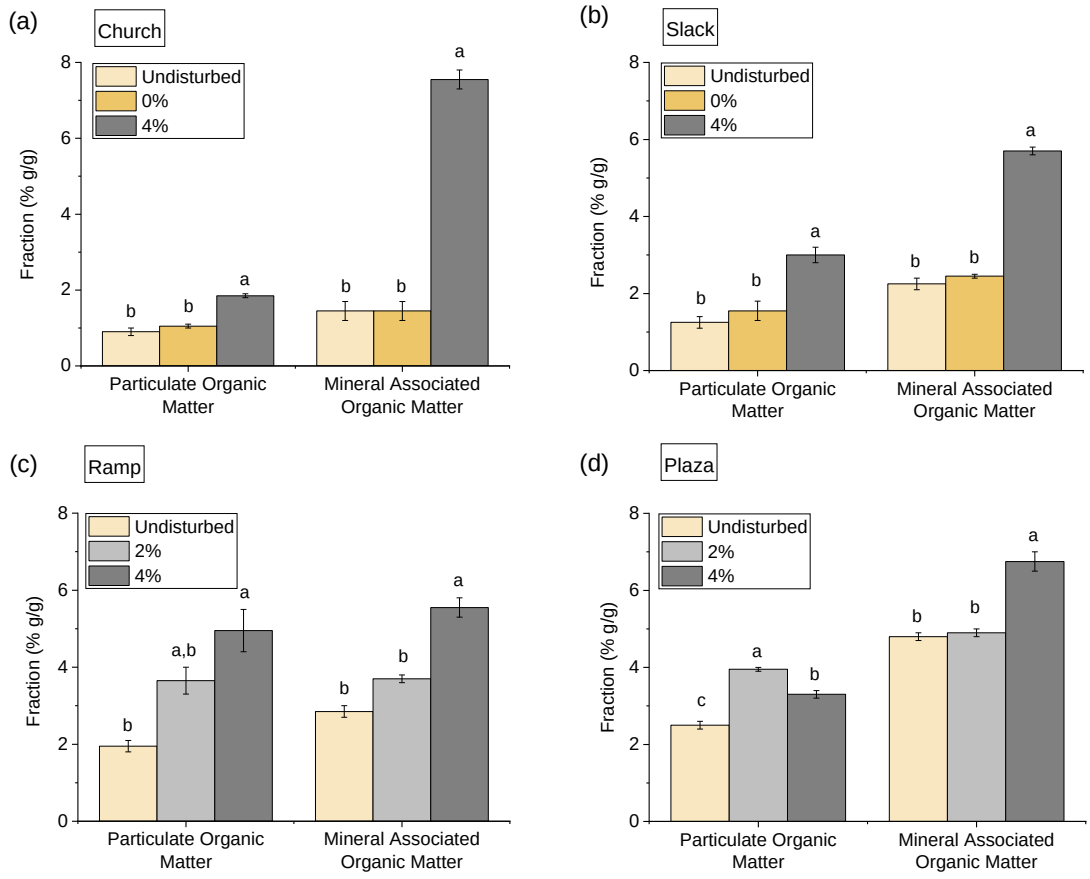


**Figure 3.5** Mean fraction (% g/g) of particulate organic matter (density < 1.8 g/cm$^3$) and mineral associated organic matter of soil samples collected from (a) Church and (b) Slack sites after 15 months of biochar amendment, and (c) Ramp and (d) Plaza sites after five months of biochar amendment. Error bars depict standard error of the means (n = 3 for all treatment). Letters denote differences using Tukey's HSD test at $\alpha = 0.05$.

## 3.5 Correlation Between Soil Compaction and Vegetation Cover with $K_{sat}$

Soil compaction was measured as the mean compaction pressure (kg/cm$^2$) in the Ramp and Plaza site soils five months following biochar amendment. Mean compaction pressure at the Ramp site for the undisturbed soil ranged from 10 ± 3 SE kg/cm$^2$ for top (10 cm depth) to 24 ± 3 SE kg/cm$^2$ for deep soil (20 to 30 cm) as shown in Figure 3.6(a).

Biochar amendment decreased the mean compaction pressure to 1.7 ± 0.7 for the top 10 cm of 4% biochar amended soil, and to 13.8 ± 0.9 kg/cm$^2$ for the 20 to 30 cm deep 2% biochar amended soil.

At the Plaza site (Figure 3.6 (b)), mean compaction pressure for the undisturbed soil ranged from 10 ± 3 kg/cm$^2$ for top (10 cm) to 24 ± 3 kg/cm$^2$ for deep soil (20 to 30 cm). Both 2% and 4% biochar amendment significantly decreased the mean compaction pressure for the top 20 cm depth at both sites. Hence, $K_{sat}$ and mean compaction pressure up to 20 cm depth were correlated with a Pearson's coefficient of 0.60 for the Ramp site biochar amended soils (Figure 3.6 (c)) and 0.98 for Plaza site amended soils (Figure 3.6(d)).

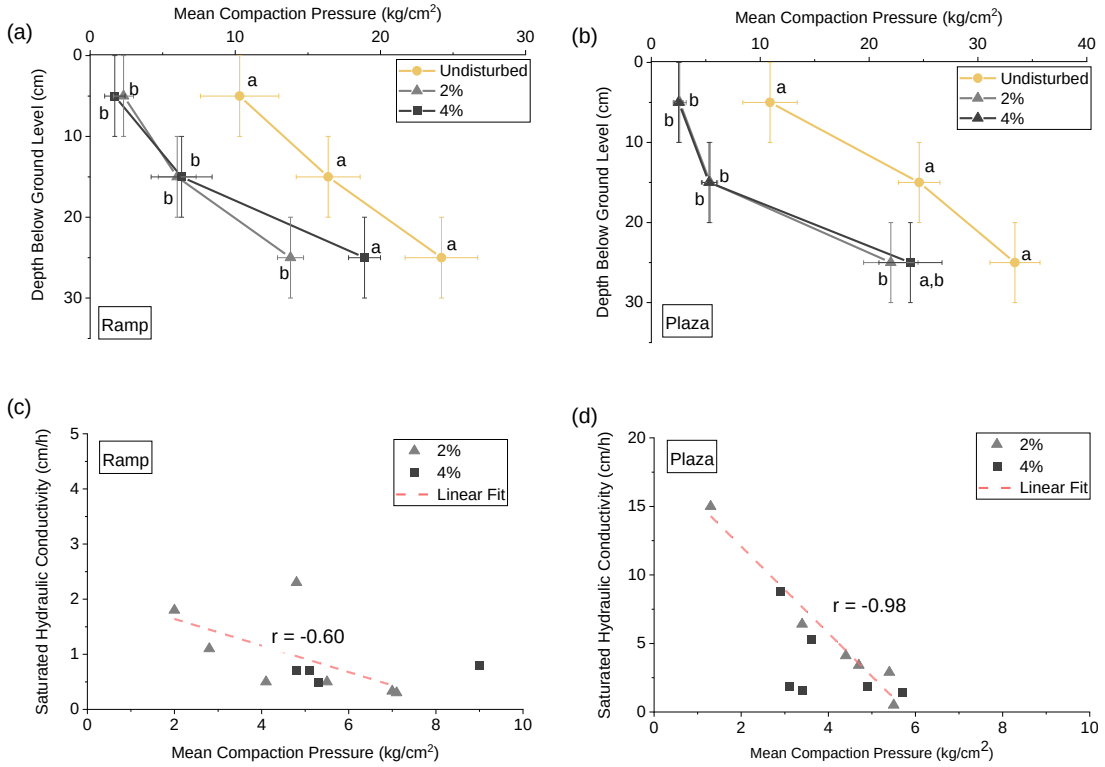


**Figure 3.6** Mean compaction pressure (kg/cm$^2$) for different soil treatments at (a) Ramp and (b) Plaza sites. Horizontal error bars represent standard error of the mean (n = 4). Vertical error bars represent the range of depths for the cone penetrometer measurements. Letters denote differences using Tukey's HSD test at $\alpha = 0.05$. Pearson's correlations are reported between saturated hydraulic conductivity (cm/h) and mean compaction pressure (kg/cm$^2$) up to 20 cm depth for the c) Ramp and (d) Plaza sites.

During July 2020, the monitoring period of the Church site, $K_{sat}$ was found to be higher in 0% amended section and adjacent undisturbed soils than the 4% biochar amended section and soils adjacent to this treatment. Close observation of vegetation at the Church site revealed that there was a difference in vegetation species between the 0% and 4% amended regions (Figure A.6). In the 4% amended soil, major vegetation species were Tall fescue grass, whereas in the 0% amended section most of the soil was densely covered with Ground ivy, White clover, along with tall fescue grass. Since the

vegetation density and species might have affect $K_{sat}$, for the Ramp and Plaza sites vegetation cover for individual $K_{sat}$ sampling regions was quantified. The correlation of $K_{sat}$ and vegetative cover showed $K_{sat}$ to be positively correlated with percent vegetative cover of the sampling area with coefficient of 0.97 for the Ramp site (Figure A.8 (a)) and 0.38 for the Plaza site (Figure A.8 (b)). However, further assessment for role of different turfgrass species, with different growth rate, root architecture, evapotranspiration rate, in controlling $K_{sat}$ is required.

# Chapter 4

# DISCUSSION

Biochar used in this study was produced from wood feedstock at high (~950$^0$C) pyrolysis temperature resulting in biochar with large particle size, high surface area, high pH, high cation exchange capacity and high aromaticity or stability (Chia et al., 2019; Xiao et al., 2018; Zhao et al., 2013). While the larger particle size, high surface area and porosity can play a key role in controlling the immediate impact on soil hydraulic conductivity and water retention (Edeh et al., 2020; Liu et al., 2017), the high pH, cation exchange capacity and aromaticity can influence stable aggregate formation and potentially the soil hydrology as soil structure evolves (Islam et al., 2021; Mukherjee & Lal, 2013). Overall, biochar amendment increased the roadway soil saturated hydraulic conductivity ($K_{sat}$) all sites, with greatest effects in the Ramp site soil, which was low in organic matter, cation exchange capacity and exchangeable cations. In addition, potential controlling factors in the field such as soil compaction and vegetation cover were correlated with the soil hydraulic conductivity. Water stored at field capacity (FC) often described as the water stored after gravity drainage was higher in biochar amended soils, On the other hand, water stored at permanent wilting point (PWP) defined as the minimum water content at which plant wilts decreased. Thus, biochar amendment increased the difference between FC and PWP defined as Plant Available Water (PAW). Such increases in plant available water in biochar amended soil indicate the potential of biochar to improve plant growth and yield, which was observed in the limited vegetation cover measurements at the Ramp and Plaza sites.

The evaluation of time dependent changes in aggregate fraction revealed that the biochar amendment increased the mean percent of total aggregate fraction with higher

mean weight diameter. Similar to hydraulic impact, the impact on stable aggregate fraction was more prominent in soil low in organic matter, cation exchange capacity and exchangeable cations along with the older soils. The higher fraction of particulate organic matter in soils collected from short time treatments compared to soils collected from aged treatments indicate that biochar is initially fragmentated distinct from other soil components but with aging is subsequently stabilized through formation of organo-mineral associates followed by aggregate formation. The increase in organo-mineral associate fraction was concurrent with the increase in stable aggregate fraction meaning that soil experiencing the highest percent increase in total aggregate fraction and mean weight of aggregation also had highest increase in organo-mineral associates compared to the undisturbed soil. Similarly, soil with similar and lowest increase in aggregate fraction also had similar or lowest increase in organo-mineral associates. Together these results support the hypothesis that biochar amendment enhances organo-mineral association and subsequently soil aggregation.

# Chapter 5

# CONCLUSIONS

In this study, the impact of a commercial wood biochar in enhancing the urban roadway soil infiltration and associated changes in soil aggregation were evaluated over time through field-scale monitoring combined with laboratory analyses. Regardless of the nature of native soil and the age of the treatment system, biochar amendment enhanced the stormwater infiltration through increased soil saturated hydraulic conductivity and water storage capacity. Laboratory analyses of undisturbed field soil cores indicated that the positive changes in soil hydraulic properties were associated with biochar induced organo-mineral association in native soil followed by increased water stable aggregate formation.

Future studies are required to investigate how biochar driven aggregation alters soil pore network with time. In addition, a predictive model should be developed for biochar impact in soil pore space and associated hydraulic properties. Since enhanced organo-mineral association initiated the biochar driven aggregation process, more study with different soil biochar mixtures to assess the magnitude and timescale of organo-mineral association formation is required. In the field, decreased soil compaction or bulk density and changes in vegetation density and species can play role in controlling soil hydraulic properties. Hence, erosion of soil-biochar mixtures associated with significantly low bulk density along with the impact of biochar on growth of vegetation and their roots, which may affect soil hydrology, should be studied.

## REFERENCES


Ahmed, F, Nestingen, R., Nieber, J. L., Gulliver, J. S., & Hozalski, R. M. (2014). A modified Philip–Dunne infiltrometer for measuring the field-saturated hydraulic conductivity of surface soil. *Vadose Zone Journal*, *13*(10), 1–14.

Ahmed, Farzana, Gulliver, J. S., & Nieber, J. L. (2015a). Field infiltration measurements in grassed roadside drainage ditches: Spatial and temporal variability. *Journal of Hydrology*, *530*, 604–611. https://doi.org/10.1016/j.jhydrol.2015.10.012

Ahmed, Farzana, Gulliver, J. S., & Nieber, J. L. (2015b). Field infiltration measurements in grassed roadside drainage ditches: Spatial and temporal variability. *Journal of Hydrology*, *530*, 604–611. https://doi.org/10.1016/j.jhydrol.2015.10.012

Bastidas, A. M. P. (2016). *Ottawa F-65 sand characterization*. University of California, Davis.

Blanco-Canqui, H. (2017). Biochar and Soil Physical Properties. *Soil Science Society of America Journal*, *81*(4), 687–711. https://doi.org/10.2136/sssaj2017.01.0017

Brodowski, S., John, B., Flessa, H., & Amelung, W. (2006). Aggregate-occluded black carbon in soil. *European Journal of Soil Science*, *57*(4), 539–546.

Bronick, C. J., & Lal, R. (2005). Soil structure and management: A review. *Geoderma*, *124*(1–2), 3–22. https://doi.org/10.1016/j.geoderma.2004.03.005

Chen, Y., Day, S. D., Wick, A. F., & McGuire, K. J. (2014a). Influence of urban land development and subsequent soil rehabilitation on soil aggregates, carbon, and hydraulic conductivity. *Science of the Total Environment*, *494–495*, 329–336. https://doi.org/10.1016/j.scitotenv.2014.06.099

Chen, Y., Day, S. D., Wick, A. F., & McGuire, K. J. (2014b). Influence of urban land development and subsequent soil rehabilitation on soil aggregates, carbon, and hydraulic conductivity. *Science of the Total Environment*, *494*, 329–336.

Chia, C. H., Downie, A., & Munroe, P. (2019). Characteristics of biochar: physical and structural properties. *Biochar for Environmental Management*, 121–142. https://doi.org/10.4324/9780203762264-12

Culpepper, T., Young, J., & Wherley, B. (2020). Comparison of four warm-season turfgrass species to natural rainfall or supplemental irrigation in a semiarid climate. *Agrosystems, Geosciences & Environment*, *3*(1), e20011.

Denef, K., Six, J., Bossuyt, H., Frey, S. D., Elliott, E. T., Merckx, R., & Paustian, K. (2001). Influence of dry–wet cycles on the interrelationship between aggregate, particulate organic matter, and microbial community dynamics. *Soil Biology and Biochemistry*, *33*(12–13), 1599–1611.

Edeh, I. G., Mašek, O., & Buss, W. (2020). A meta-analysis on biochar's effects on soil water properties – New insights and future research challenges. *Science of the Total Environment*, *714*. https://doi.org/10.1016/j.scitotenv.2020.136857

Islam, M. U., Jiang, F., Guo, Z., & Peng, X. (2021). Does biochar application improve soil aggregation? A meta-analysis. *Soil and Tillage Research*, *209*, 104926.

Joseph, S. D., Camps-Arbestain, M., Lin, Y., Munroe, P., Chia, C. H., Hook, J., Van Zwieten, L., Kimber, S., Cowie, A., Singh, B. P., Lehmann, J., Foidl, N., Smernik, R. J., & Amonette, J. E. (2010). An investigation into the reactions of biochar in soil. *Australian Journal of Soil Research*, *48*(6–7), 501–515. https://doi.org/10.1071/SR10009

Karcher, D. E., & Richardson, M. D. (2005). Batch analysis of digital images to evaluate turfgrass characteristics. *Crop Science*, *45*(4), 1536–1539.

Kelly, C. N., Benjamin, J., Calderon, F. C., Mikha, M. M., Rutherford, D. W., & Rostad, C. E. (2017). Incorporation of biochar carbon into stable soil aggregates: the role of clay mineralogy and other soil characteristics. *Pedosphere*, *27*(4), 694–704.

Korres, N. E., Norsworthy, J. K., & Mauromoustakos, A. (2019). Effects of Palmer amaranth (Amaranthus palmeri) establishment time and distance from the crop row on biological and phenological characteristics of the weed: implications on soybean yield. *Weed Science*, *67*(1), 126–135.

Leong, E. C., Tripathy, S., & Rahardjo, H. (2004). A modified pressure plate apparatus. *Geotechnical Testing Journal*, *27*(3), 322–331.

Lim, T. J., Spokas, K. A., Feyereisen, G., & Novak, J. M. (2016). Predicting the impact of biochar additions on soil hydraulic properties. *Chemosphere*, *142*, 136–144. https://doi.org/10.1016/j.chemosphere.2015.06.069

Liu, Z., Dugan, B., Masiello, C. A., Barnes, R. T., Gallagher, M. E., & Gonnermann, H. (2016). Impacts of biochar concentration and particle size on hydraulic conductivity and DOC leaching of biochar–sand mixtures. *Journal of Hydrology*, *533*, 461–472.

Liu, Z., Dugan, B., Masiello, C. A., & Gonnermann, H. M. (2017). Biochar particle size, shape, and porosity act together to influence soil water properties. *Plos One*, *12*(6),

e0179079.

Masiello, C., Dugan, B., Brewer, C., Spokas, K., Novak, J., Liu, Z. (2015). Biochar effects on soil hydrology. *Biochar for Environmental Management, Science, Technology and Implementation*, 543–562.

Mukherjee, A., & Lal, R. (2013). Biochar Impacts on Soil Physical Properties and Greenhouse Gas Emissions. *Agronomy*, *3*(2), 313–339. https://doi.org/10.3390/agronomy3020313

Nakhli, S. A. A., Goy, S., Manahiloh, K. N., & Imhoff, P. T. (2021). Spatial heterogeneity of biochar (segregation) in biochar-amended media: An overlooked phenomenon, and its impact on saturated hydraulic conductivity. *Journal of Environmental Management*, *279*, 111588.

Nakhli, S. A. A., Tian, J., & Imhoff, P. T. (2021). Preparing and characterizing repacked columns for experiments in biochar-amended soils. *MethodsX*, *8*, 101205.

Oades, J. M., & Waters, A. G. (1991). Aggregate hierarchy in soils. *Soil Research*, *29*(6), 815–828.

Obia, A., Mulder, J., Martinsen, V., Cornelissen, G., & Børresen, T. (2016). In situ effects of biochar on aggregation, water retention and porosity in light-textured tropical soils. *Soil and Tillage Research*, *155*, 35–44.

Olson, N. C., Gulliver, J. S., Nieber, J. L., & Kayhanian, M. (2013). Remediation to improve infiltration into compact soils. *Journal of Environmental Management*, *117*, 85–95. https://doi.org/10.1016/j.jenvman.2012.10.057

Omondi, M. O., Xia, X., Nahayo, A., Liu, X., Korai, P. K., & Pan, G. (2016). Quantification of biochar effects on soil hydrological properties using meta-analysis of literature data. *Geoderma*, *274*, 28–34. https://doi.org/10.1016/j.geoderma.2016.03.029

Parra Bastidas, A. M., Boulanger, R. W., Carey, T. J., & DeJong, J. T. (2016). Ottawa F-65 sand data from Ana Maria Parra Bastidas. *NEEShub, Http://Dx. Doi. Org/10.17603/DS2MW2R*.

Pignatello, J. J., Uchimiya, M., Abiven, S., & Schmidt, M. W. I. (2019). Evolution of biochar properties in soil. *Biochar for Environmental Management*, 227–266. https://doi.org/10.4324/9780203762264-16

Pitt, R., Asce, M., Chen, S., Asce, A. M., Clark, S. E., Asce, M., Swenson, J., Asce, A. M., Ong, C. K., & Asce, A. M. (2009). *Compaction ' s Impacts on Urban Storm-*

*Water Infiltration*. *134*(5), 652–658.

Pronk, G. J., Heister, K., Ding, G.-C., Smalla, K., & Kögel-Knabner, I. (2012). Development of biogeochemical interfaces in an artificial soil incubation experiment; aggregation and formation of organo-mineral associations. *Geoderma*, *189*, 585–594.

Rahman, M. T., Guo, Z. C., Zhang, Z. B., Zhou, H., & Peng, X. H. (2018). Wetting and drying cycles improving aggregation and associated C stabilization differently after straw or biochar incorporated into a Vertisol. *Soil and Tillage Research*, *175*, 28–36.

Regelink, I. C., Stoof, C. R., Rousseva, S., Weng, L., Lair, G. J., Kram, P., Nikolaidis, N. P., Kercheva, M., Banwart, S., & Comans, R. N. J. (2015). Linkages between aggregate formation, porosity and soil chemical properties. *Geoderma*, *247–248*, 24–37. https://doi.org/10.1016/j.geoderma.2015.01.022

Russell, T. R., Karcher, D. E., & Richardson, M. D. (2019). Daily light integral requirement of a creeping bentgrass putting green as affected by shade, trinexapac-ethyl, and a plant colorant. *Crop Science*, *59*(4), 1768–1778.

Six, J., Elliott, E. T., Paustian, K., & Doran, J. W. (1998). Aggregation and soil organic matter accumulation in cultivated and native grassland soils. *Soil Science Society of America Journal*, *62*(5), 1367–1377.

Tisdall, J. M., & OADES, J. M. (1982). Organic matter and water-stable aggregates in soils. *Journal of Soil Science*, *33*(2), 141–163.

Vasko, A. (2015). *An investigation into the behavior of Ottawa sand through monotonic and cyclic shear tests*. The George Washington University.

Voter, C. B., & Loheide, S. P. (2018). Urban residential surface and subsurface hydrology: synergistic effects of low-impact features at the parcel scale. *Water Resources Research*, *54*(10), 8216–8233.

Wanniarachchi, Cheema, Thomas, & Galagedara. (2019). Effect of Biochar on TDR-Based Volumetric Soil Moisture Measurements in a Loamy Sand Podzolic Soil. *Soil Systems*, *3*(3), 49. https://doi.org/10.3390/soilsystems3030049

Wick, A. F., Ingram, L. J., & Stahl, P. D. (2009). Aggregate and organic matter dynamics in reclaimed soils as indicated by stable carbon isotopes. *Soil Biology and Biochemistry*, *41*(2), 201–209.

Xiao, X., Chen, B., Chen, Z., Zhu, L., & Schnoor, J. L. (2018). Insight into multiple and

multilevel structures of biochars and their potential environmental applications: a critical review. *Environmental Science & Technology*, *52*(9), 5027–5047.

Yang, F., Zhao, L., Gao, B., Xu, X., & Cao, X. (2016). The interfacial behavior between biochar and soil minerals and its effect on biochar stability. *Environmental Science & Technology*, *50*(5), 2264–2271.

Zhang, Q., Song, Y., Wu, Z., Yan, X., Gunina, A., Kuzyakov, Y., & Xiong, Z. (2020). Effects of six-year biochar amendment on soil aggregation, crop growth, and nitrogen and phosphorus use efficiencies in a rice-wheat rotation. *Journal of Cleaner Production*, *242*, 118435.

Zhang, Z., Lin, L., Wang, Y., & Peng, X. (2016). Temporal change in soil macropores measured using tension infiltrometer under different land uses and slope positions in subtropical China. *Journal of Soils and Sediments*, *16*(3), 854–863.

Zhao, L., Cao, X., Mašek, O., & Zimmerman, A. (2013). Heterogeneity of biochar properties as a function of feedstock sources and production temperatures. *Journal of Hazardous Materials*, *256*, 1–9.

Zheng, H., Wang, X., Luo, X., Wang, Z., & Xing, B. (2018). Biochar-induced negative carbon mineralization priming effects in a coastal wetland soil: roles of soil aggregation and microbial modulation. *Science of the Total Environment*, *610*, 951–960.

# Appendix A

## SUPPLEMENTARY FIGURES AND TABLES

(a)

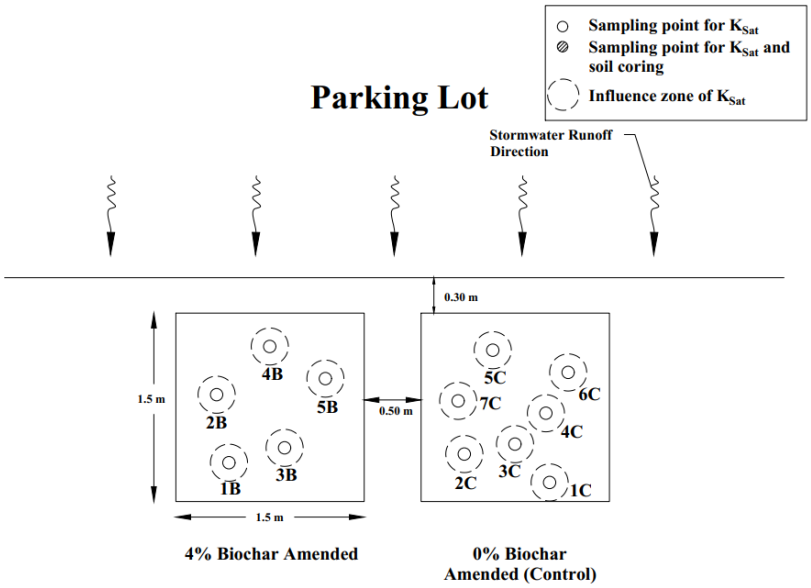


(b)

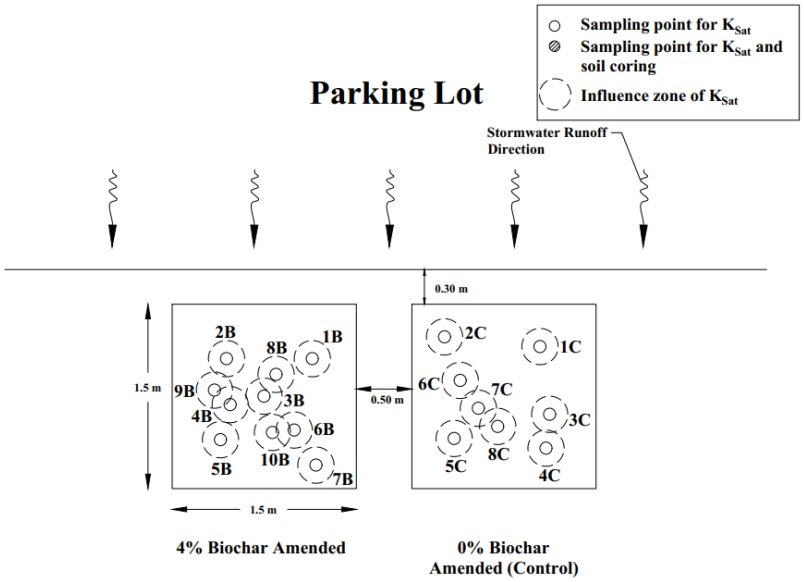


**Figure A.1** Site plan showing field monitoring of $K_{sat}$. Measurements during September 2019 for (a) Church Site and (b) Slack Site. Numbers indicate sampling points. Letters indicate different treatment section: U = undisturbed, C = 0% biochar amended(control), and B = 4% biochar amended.

(a)

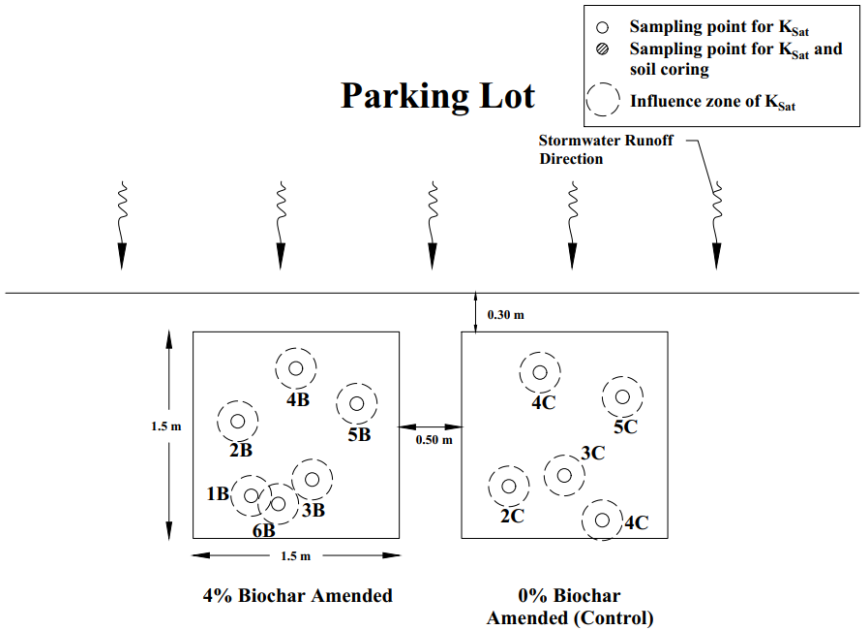


(b)

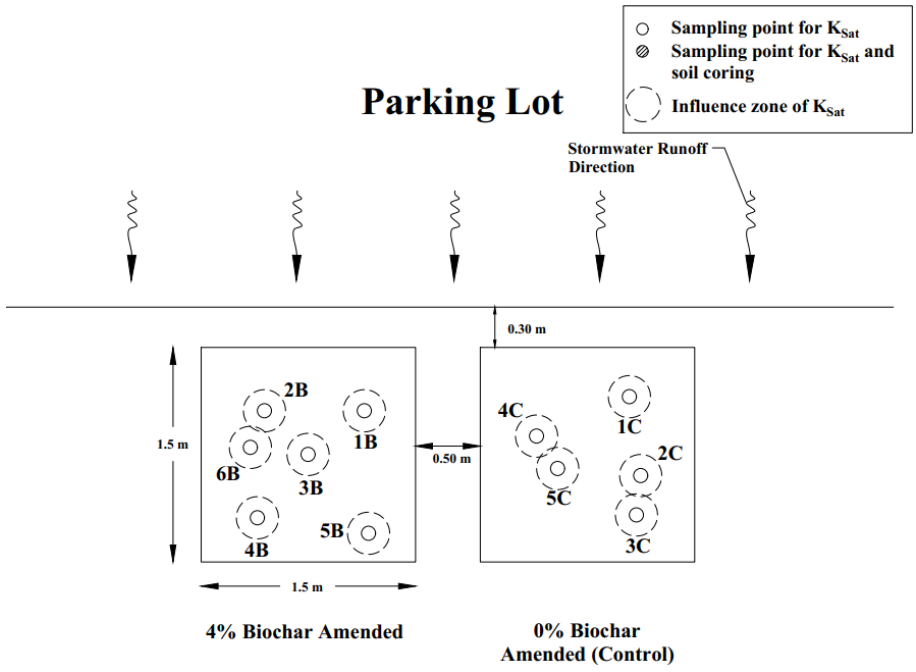


**Figure A.2** Site plan showing field monitoring of $K_{sat}$. Measurements during November 2019 for (a) Church Site and (b) Slack Site. Numbers indicate sampling points. Letters indicate different treatment section: U = undisturbed, C = 0% biochar amended(control), and B = 4% biochar amended.

(a)

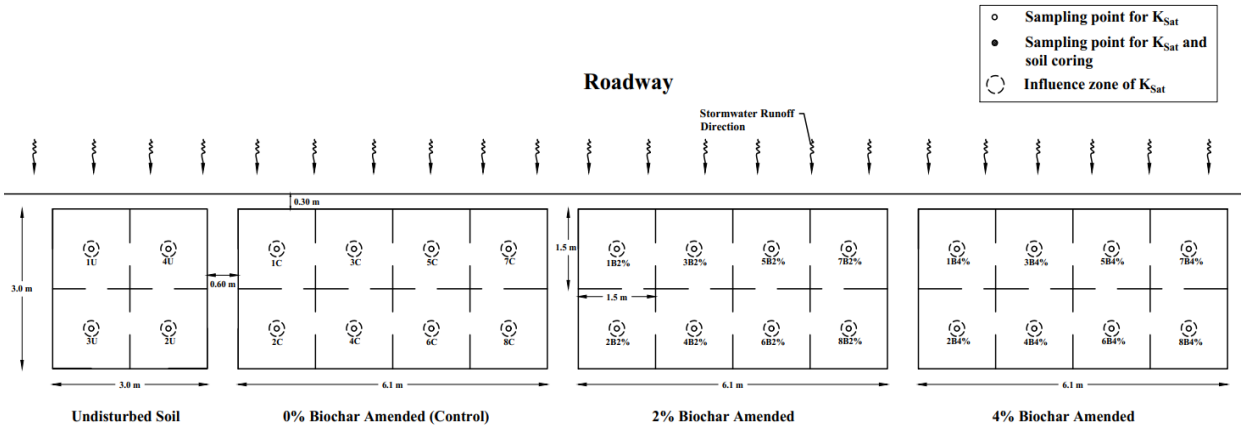


(b)

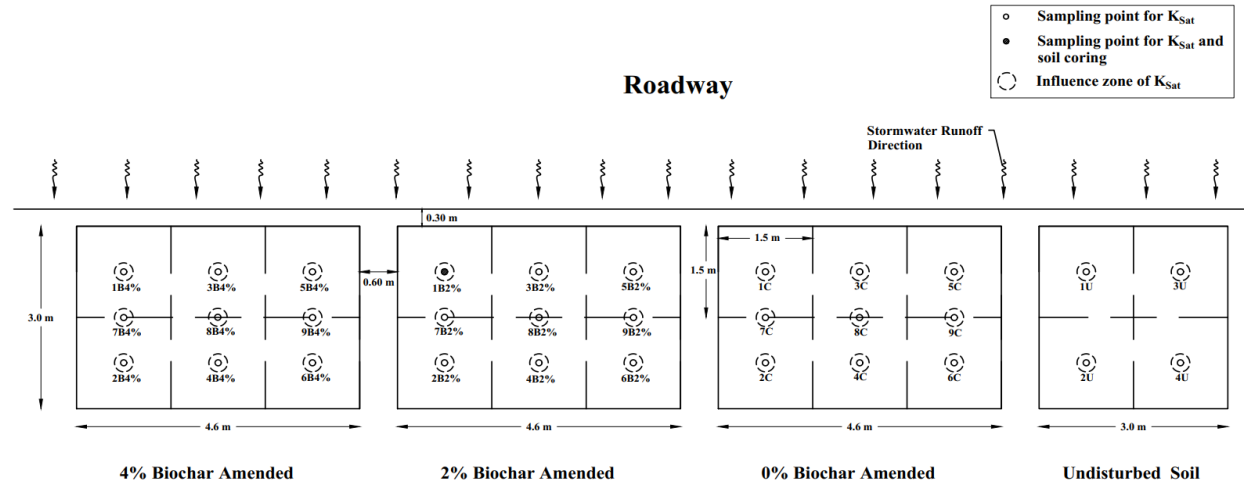


**Figure A.3** Site plan showing field monitoring of $K_{sat}$ during November 2020 for (a) Ramp and (b) Plaza Sites. Numbers denote sampling points. Letters denote different treatment section: U = undisturbed, C = 0% biochar amended (control), B2% = 2% biochar amended, and B4% = 4% biochar amended.

**Table A.1** Summary results of field $K_{sat}$ measurements

| Site | Monitoring Period | Treatment Section | Geometric mean of $K_{sat}$ (cm/h) | Coefficient of variation of $K_{sat}$ (cm/h) | Ratio of Geometric mean $K_{sat}$ (cm/h) | |
|---|---|---|---|---|---|---|
| | | | | | $K_{sat\text{-}Undisturbed}$/ $K_{sat\text{-}Treated\ (0\%\ or\ 2\%\ or\ 4\%)}$ | $K_{sat\text{-}0\%\ or\ 2\%}$ / $K_{sat\text{-}4\%}$ |
| **Church** | September 2019 | 0% | 1.20 | 0.72 | - | 1.8 |
| | | 4% | 2.16 | 0.78 | - | |
| | November 2019 | 0% | 0.40 | 0.17 | - | 2.1 |
| | | 4% | 0.85 | 0.72 | - | |
| | July 2020 | Undisturbed (near 0%) | 1.84 | 0.46 | - | - |
| | | Undisturbed (near 4%) | 0.35 | 0.10 | - | - |
| | | 0% | 2.20 | 0.59 | 1.2 | 0.7 |
| | | 4% | 1.61 | 0.55 | 4.6 | |
| **Slack** | September 2019 | 0% | 8.84 | 0.59 | - | 5.3 |
| | | 4% | 47.12 | 0.55 | - | |
| | November 2019 | 0% | 4.72 | 0.47 | - | 1.8 |
| | | 4% | 8.54 | 0.17 | - | |
| | July 2020 | Undisturbed | 15.76 | 0.74 | - | - |
| | | 0% | 1.15 | 1.23 | 0.1 | 9.3 |
| | | 4% | 10.71 | 0.74 | 0.7 | |
| **Ramp** | August 2020 | Undisturbed | < 0.3 | - | - | - |
| | | 2% | 8.47 | 1.8 | 28.2 | 1.9 |
| | | 4% | 16.84 | 1.5 | 56.1 | |
| | November 2020 | Undisturbed | < 0.3 | - | - | - |
| | | 2% | 1.30 | 2.5 | 4.3 | 3.5 |
| | | 4% | 4.54 | 1.2 | 15.1 | |
| **Plaza** | August 2020 | Undisturbed | 3.55 | 0.8 | - | - |
| | | 2% | 38.63 | 0.4 | 10.9 | 0.8 |
| | | 4% | 30.20 | 0.4 | 8.5 | |
| | November 2020 | Undisturbed | 0.64 | 1.2 | - | - |
| | | 2% | 2.35 | 1.0 | 3.7 | 1.4 |
| | | 4% | 3.35 | 0.9 | 5.2 | |

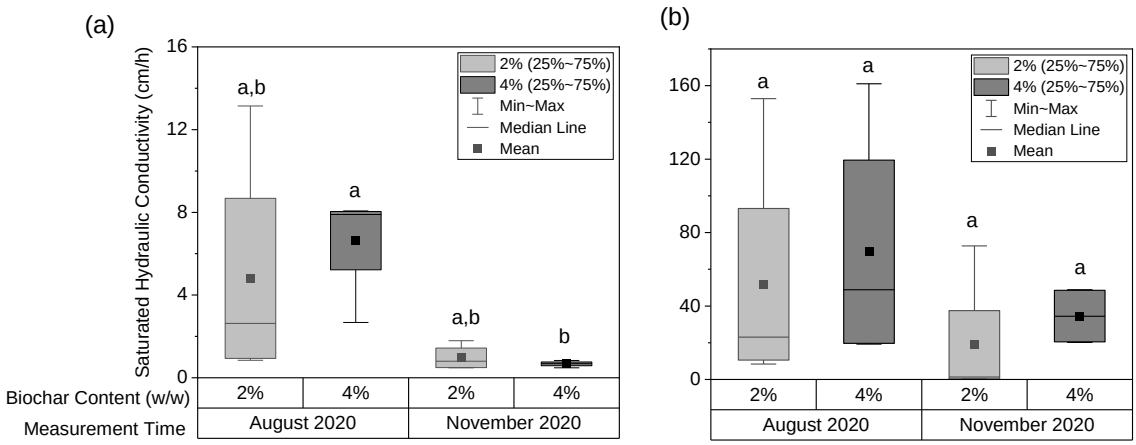


**Figure A.4** Box plot showing field saturated hydraulic conductivity (cm/h) at different monitoring periods for Ramp site: (a) Upslope sampling points, and (b) Downslope sampling points. Letters denote differences using Tukey's HSD test at $\alpha = 0.05$.

**Table A.2** Comparison between upslope and downslope field $K_{sat}$ (cm/h) of Ramp site.

| **Monitoring Period** | **Treatment Section** | | **Geometric mean of $K_{sat}$ (cm/h)** | $K_{sat\text{- }Upslope} / K_{sat\text{-}Downslope}$ |
|---|---|---|---|---|
| August 2020 | 2% | Upslope | 2.63 | 10.3 |
| | | Downslope | 27.16 | |
| | 4% | Upslope | 6.05 | 7.7 |
| | | Downslope | 46.87 | |
| November 2020 | 2% | Upslope | 0.83 | 2.4 |
| | | Downslope | 2.02 | |
| | 4% | Upslope | 0.66 | 47.7 |
| | | Downslope | 31.50 | |

(a)

(b)

**Figure A.5** Field site view of (a) 0% amended section and (b) 4% amended section in Ramp site during August 2020.

(a)

(b)

**Figure A.6** Field site view of (a) 0% amended section (b) 4% amended section in Church site during July 2020.

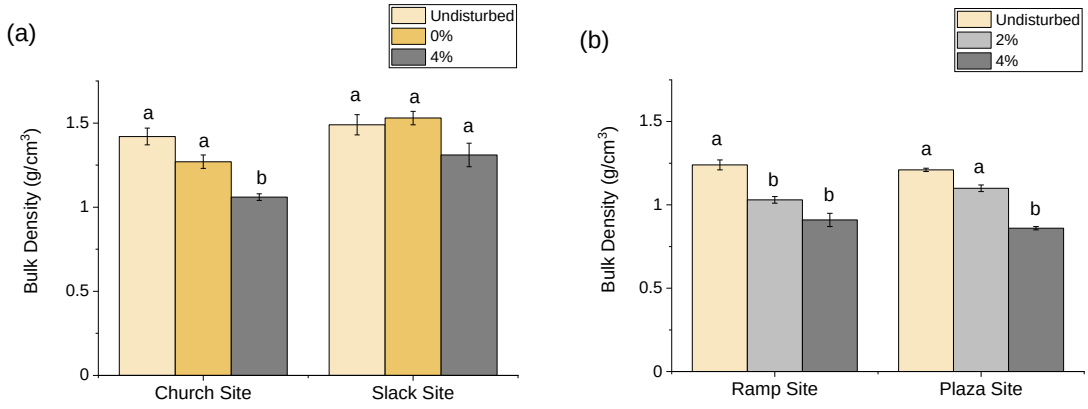


**Figure A.7** Mean bulk density (g/cm$^3$) of soil samples collected from (a) Church and Slack site after 15 months of biochar amendment, and (b) Ramp and Plaza site after five months of biochar amendment. Error bars depict standard error of the means (n = 3 for all treatment). Letters denote differences using Tukey's HSD test at $\alpha = 0.05$.

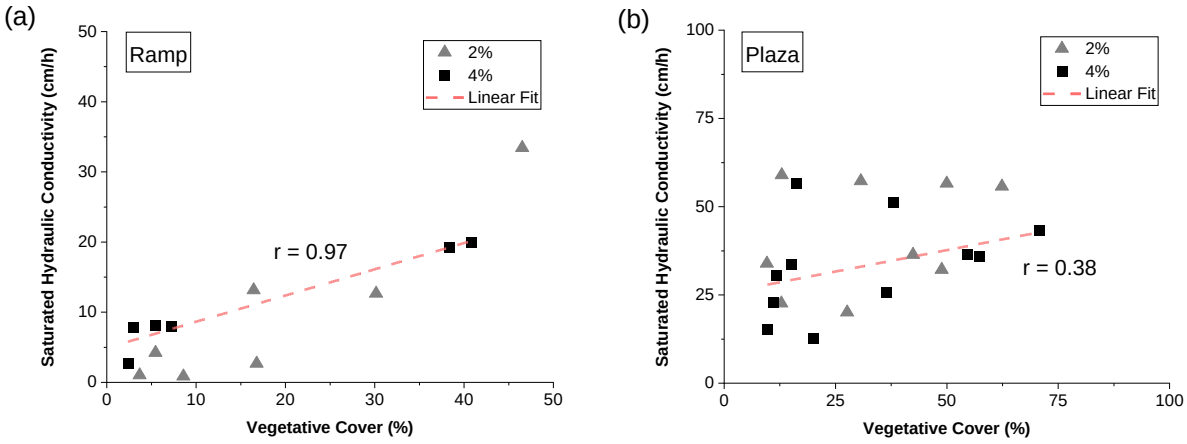


**Figure A.8** Correlation between saturated hydraulic conductivity (cm/h) and percent vegetative cover for (a) Ramp and (b) Plaza site soils

# Appendix B

# TESTING OF MPD ACCURACY

## B.1 Design of Test for MPD Accuracy

Ottowa F-65 sand was used to test the accuracy of hydraulic conductivity measurements using MPD in a laboratory setup. For the test, a certain mass (kg) of the dry sand was packed up to a specific height of a bucket (30 cm in diameter and 50 cm in height) to achieve a desired bulk density. Once packed, the MPD cylinder was placed on the top surface of the sand (Figure B.1) and filled with water. The change in water level in cylinder with time was recorded until all water was drained into the sand. The final VWC (%) of the packed sand was measured using time domain reflectometry (TDR 150).

**Figure B.1** Test setup for MPD accuracy

The wet sand was mixed homogeneously in a large tray and was packed in the bucket at different dry bulk density to test with different initial VWC (5% followed by 13%). Using the initial VWC and final VWC and water head vs time data, hydraulic conductivity was calculated using MPD analysis spreadsheet. In this way a set of tests was performed with the Ottowa F-65 sand with different initial VWC (%) packed at different dry bulk densities. For all tests, maximum diameter for zone of influence for MPD was 24 cm which was less than the diameter of the bucket used for the tests.

## B.2 Results of Test for MPD Accuracy

The hydraulic conductivity values measured using MPD were compared with the values reported by different researchers for this sand as shown in Table B.1 and Figure B.2.

**Table B.1** Summary results of hydraulic conductivity test with Ottowa F-65 sand

| **Measured using MPD** | | | | | **Reported by other Researchers** | | |
|---|---|---|---|---|---|---|---|
| **Test** | **Initial VWC (%)** | **Final VWC (%)** | **Dry Bulk Density ($kg/m^3$)** | **Hydraulic Conductivity (cm/s)** | **Dry Bulk Density ($kg/m^3$)** | **Hydraulic Conductivity (cm/s)** | **Author** |
| 1 | 0 | 36 | 1694 | 0.0157 | 1480 | 0.022 | Parra et al., 2016 |
| 2 | 0 | 36 | 1715.7 | 0.0145 | 1722 | 0.016 | |
| 3 | 0 | 36 | 1716.4 | 0.0142 | 1654 | 0.017 | Parra et al., 2016 |
| 4 | 5 | 38 | 1576.8 | 0.0265 | 1537 | 0.0164 | Vasko et al., 2015 |
| 5 | 5 | 38 | 1647.4 | 0.0226 | 1617 | 0.0118 | |
| 6 | 13 | 42 | 1760 | 0.0166 | | | |

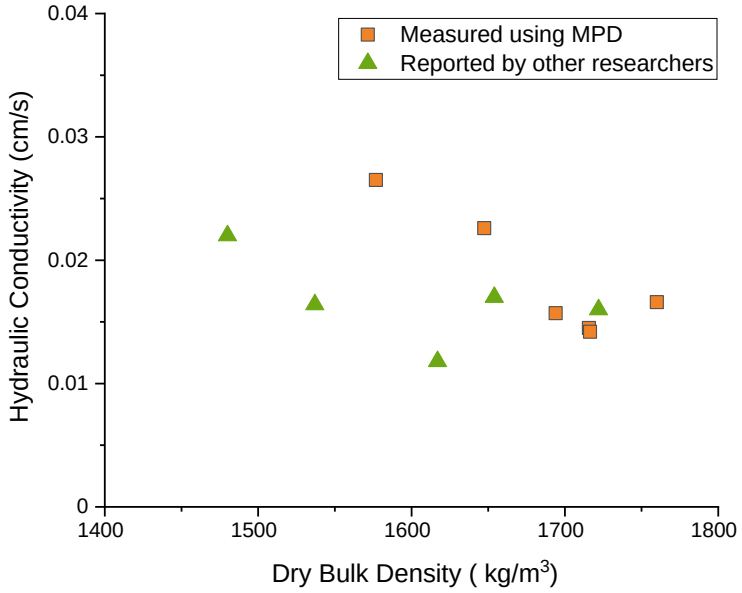


**Figure B.2** Hydraulic Conductivity of Ottowa F-65 sand for different dry bulk density